University POLITEHNICA of Bucharest
Faculty of Chemical Engineering and Biotechnologies
Department of Science and Engineering of Oxide Materials and Nanomaterials

PhD THESIS - SUMMARY

Biodegradable antimicrobial packaging

Scientific coordinator:
Prof. Dr. Eng. Habil. Anton FICAI

PhD student:
Eng. Ludmila MOTELICA

BUCHAREST
2022

Keywords: Antibacterial packaging, biodegradable, alginate film, chitosan film, citronella essential oil, zinc oxide nanoparticles, silver nanoparticles.

Contents

List of Abbreviations

A-Alginate
AZ- Alginate/ZnO
AA- Alginate/Ag
AAZ- Alginate/Ag/ZnO
ANOVA – Analysis of Variance
ATR – Attenuation of total reflection
C-Chitosan
CZ – Chitosan/ZnO
CA – Chitosan/Ag
CZA – Chitosan/ZnO/Ag
CEO – Citronella essential oil
CAI – Isocyanates
EDX - Energy dispersive x-ray spectroscopy
FDA - Food and drug administration
FAO - Food and agriculture organization
FTIR – Fourier transform infrared spectroscopy
GPS - Global positioning satellite system
GRAS – Generally recognized a safe
HRTEM- High resolution transmission electron microscopy
LDPE – Low-density polyethylene
LBL – Layer-by-layer
MAP – Modified atmosphere packaging
NPs – Nanoparticle
PVC – Polyvinyl chloride
PLA – Polylactic acid
PCL - Polycarprolactone
PVA – Polyvinyl alcohols
PVP – Polyvinyl pyrrolidone
PET – Polyethylene terephthalate
PEG – Polyethylene glycol
PE – Polythene
PP – Polypropylene
PL – Photoluminescence
RFID - Radio frequency identification
SPB – Sulfopropyl betaine
SSA - Sulfosuccinic
SEM – Scanning electron microscopy
SAED – Selected area electron diffraction
TTIs - Time temperature indicators
TEM – Transmission electron microscopy
TGA – Thermo-gravimetric analysis
UV-Vis – Ultraviolet-visible spectroscopy
WVP - Water vapor permeability
XRD – Powder X-ray diffraction

Introduction

The Food and Agriculture Organization (FAO) of the United Nations statistical data present a worrying picture about the food security. The released data indicate that approximatively 33% of produced food is wasted or lost year after year because of expiration, organoleptic alteration or due to decay induced by bacterial and fungal activity. Food is wasted at all levels (harvesting, storage, processing and commercialization) – Figure 1.

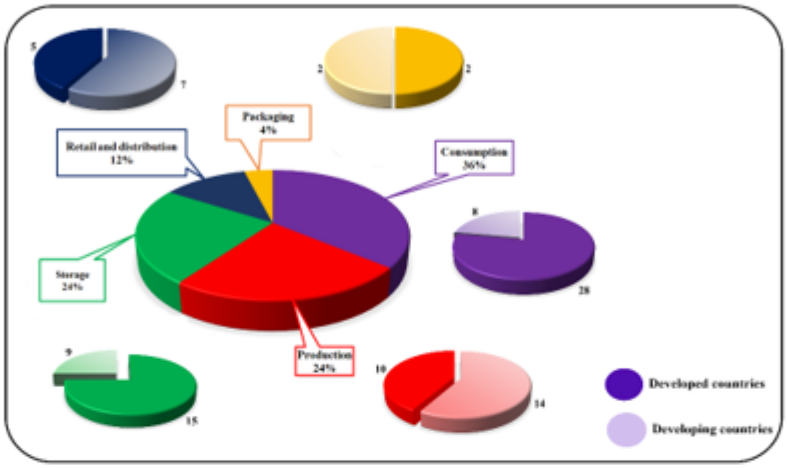

Figure 1. Food wasted at all levels of life cycle assessment

The degree of lost products varies between food categories, with fruits and vegetables leading with approximatively 45%, followed by the marine products and grains with roughly one third and dairy and meat products with one fifth of the total production. The principal cause leading to these loses is the oxidation and other degradative processes promoted by the presence of various microbial strain and enzymes. The losses are not divided equally among the countries. The less developed countries lack of adequate infrastructure. This leads to 40% losses at and after harvest process. At the same time 40% of losses are incurred at retail phase in developed countries [1].

At the customer part, huge quantities are lost because the non-natural importance place on external aspect [1]. Generally speaking, the term "loss" indicate the production or processing phases, while the term "waste" implies the distribution chain up to the consumer [2, 3].

The purpose of the doctoral thesis

The principal role of the packaging material in food industry is to protect the content from the environment. This may include the blocking of dust, water vapors, bacteria and fungi but also other unwanted chemicals that might be used in the processing or transport phase. The packaging must also protect the food further on to the shop level or after purchase, at customer level. In all these steps, the packaging must protect the food and keep it safe, with the desired quality. For these reasons, the materials used in packaging industry should be food-safe, non-reactive in the above-mentioned conditions, as cheap as possible and easy to handle and recycled.

This research provides some simple solutions that can impart some desired properties like antibacterial or antifungal activity to the packaging films. Such traits can come from the polymeric blends used for the packaging films or can be induced by the use of additionally antimicrobials. Such agents can be natural extracts like essential oils or synthetic like metallic or oxide nanoparticles. Combining multiple antimicrobials like metallic silver nanoparticles with zinc oxide nanoparticles can generate new, more potent materials, with synergic activity of components. The antibacterial and antifungal activities of a packaging material can be a function of surface coating or it can be induced in the bulk material.

The research studies underlying this PhD are focused on the processes from obtaining of bio-friendly food packaging from natural biopolymers like chitosan or alginate, with synergic antimicrobial activity bestowed by inorganic nanoparticles like ZnO or Ag, loaded with essential oils.

Natural extracts from plants present a hot topic for their high capacity to act as antibacterial and antifungal agents, but also for their antioxidant activity [32-34]. Such potent extract is represented the essential oil of citronella or lemongrass (CEO). The CEO composition is complex and depends on the harvest region, but usually contains citronellol and citronellal, that together with geraniol forms the bulk of the components [35]. In US the FDA considers CEO as a biopesticide, that has no toxicity [36]. In addition, a potent antifungal capacity is reported by literature [37].

Another well-known antimicrobial agent is the silver metallic nanoparticles (Ag NPs). The high versatility of these nanoparticles can be seen from the fact that more than 600 bacterial/fungal strains are documented to be susceptible. Numerous studies indicate that some physical characteristics, like shape or size of the silver nanoparticles, strongly influence the activity [38].

The zinc oxide antimicrobial activity is a topic of hot debate. The antibacterial capacity is well establish, but at the same time the antimycotic capacity not so often put forward in current researches [39]. As the zinc oxide presents a strong photocatalytic activity, the antimicrobial capacity is strongly related with the light presence. This implies the existence of various reactive oxygen species (ROS). The particular concentration and production speed of ROS is responsible for the damages to the cellular membrane by induced oxidative stress. An alternative pathway exists as the zinc oxide can exhibit the antimicrobial activity also in the dark. Most probably it involves some kind of mechanical puncture of the membrane, internalization of the nanoparticles and destruction of the microbial cell [40].

Enhancing the mechanical properties of the packaging films is obtained by the use of plasticizers. Glycerol is one of the wide used substances in the class of plasticizers due to its good compatibility with polysaccharides like alginate, chitosan and cellulose [41]. A reinforce of the packaging films can be obtained by cross-linking the polymeric chains with the help of various nanoparticles such as zinc oxide or silver. While the plasticizer like glycerol will act as a spacer between polymeric chains and therefore will permit an easier passage for water molecules, increasing the water vapor permeability (WVP), some other substances like zinc oxide nanoparticles or the oily natural extracts are hydrophobic in their nature so they will improve the barrier properties of the packaging [42-44]. The nanoparticles are impermeable to the water therefore they behave as a solid wall, making a tortuous pathway like a labyrinth for any molecule, be it water, CO_2, C_2H_4 or O_2 [45, 46].

I. CRITICAL STUDY OF THE LITERATURE DATA

Chapter 1. Active and smart packaging solutions in food industry

1.1. Active and intelligent packaging

The traditional main role of the packaging is to prolong the shelf life and to protect as an inert shield the food from the external factors. The next step in food industry evolution is the engineering of the active packaging which comes as a response to the increasing demands of customers and modern society. Therefore, to be classified as an active type, the packaging must fulfill some additional functions when compared with the simple traditional one [47].

Figure 2. Intelligent and active packaging functions

These types of packaging can be divided into two main categories (Figure 2):

- Active packaging are those incorporating additives (or attached to the packaging) that can maintain quality and prolong the shelf life.
- Smart packaging that monitors the properties of packaged foods and brings information to all interested parts, from consumers to retailers on the specific state of the product. E.g., RFID tags and microchips or time-temperature indicators (TTIs) – Table 1.

Beside water content, another important factor in food shelf life is the storage temperature. The temperature oscillations can induce modifications into the food and therefore alter its properties and shelf life. An effective tool in monitoring the temperature variation in time, the TTIs are mostly used for sensible products frozen or refrigerated [52].

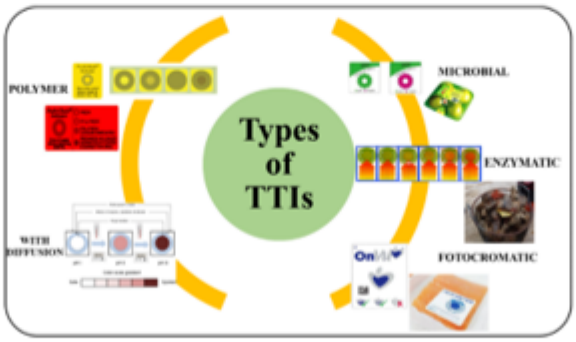

Figure 3. Types of time-temperature indicators (TTIs)

TTIs provide a visual indication that storage conditions were optimum or how long the product was exposed to increased temperatures [53]. The working principles of such indicators are based on the identification of permanent responses in enzymatic, electronic, chemical form, of nanoparticles or generated by changes in biological systems during expose to increase temperature (at or above room temperature) (Figure 3) [20].

1.2. Modified atmosphere packaging (MAP)

Various interactions processes can change the gas composition inside the package that can affect the food quality. Toxic gaseous component production inside the packaging can be monitored by useful indicators [62]. The monitoring of the chemical changes produced in the composition packaging gases is performed by changing the color of the indicator embedded in it, a change generated by an enzymatic or chemical process. By breaking the seal the label become activated and the reaction is started, the color changing over time [51].

Generating CO_2 inside the package is a popular solution that can be classified as active packaging. This is also an antimicrobial solution. Elevated quantities of CO_2, between 10 and 80% can preserve the meat products of any kind, by decreasing the bacterial colony spread on the food surface and prolong the shelf life [63].

The Ageless-eye™ indicator developed by Mitsubishi (Figure 5) can be used to monitor the oxygen level in an enclosure. If the oxygen level is below 0.1%, the indicator is light pinkish. If the oxygen concentration rises above 0.5%, the indicator changes to bright violet.

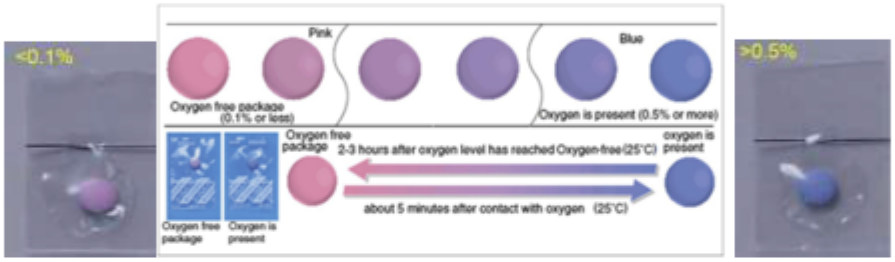

Figure 5. "Ageless-eye" indicator for the presence of more than 0.5% oxygen in a package [66]

In conclusion, the rising standards together with the significant research break-through made developing of some advanced materials possible with low cost and better performances. These advances can be seen in the field of food industry. Is noteworthy that traditionally, food packaging materials have evolved greatly, from an inactive, inert blocking material to active packaging. This new type can be loaded or coated with various nanostructures or antioxidants or even probiotics. Next natural step is the developing of hybrid materials for packaging, that exhibit several ways to interact with food and prolong shelf life while improving the quality. By introducing nanomaterials into the packaging industry, loaded with antimicrobial agents, an optimization of these features will be made.

1.3. Strategies to develop antimicrobial packaging

A simple classification of the antimicrobial materials used as packaging will identify two types. First type of materials comes in intimate contact with the food's surface, so there is a possibility that the antibacterial substances will migrate into the food. Usually the food products that are vacuum-packed can fall in this category. In the 2nd material type used for packaging the food is not making a direct contact with the film surface and here we can give as example the MAP [20, 51, 55].

For larger quantities of food, transport in textile bags (flour, sugar, potatoes, beans, etc.) is preferred. Consequently, there is research to produce fabrics with antibacterial and antifungal activity (which may have uses outside the food industry, such as in the textile industry). One of

the methods mentioned in the literature is the treatment of the cotton cloth with compounds that contains sulfopropylbetaine (SPB) and isocyanate (CAI) groups (ammonium salts), by immersing in a solution followed by drying process. Both groups can bind to the cotton fibers cloth by covalently interactions and give it excellent bactericidal and antifungal properties (Figure 6).

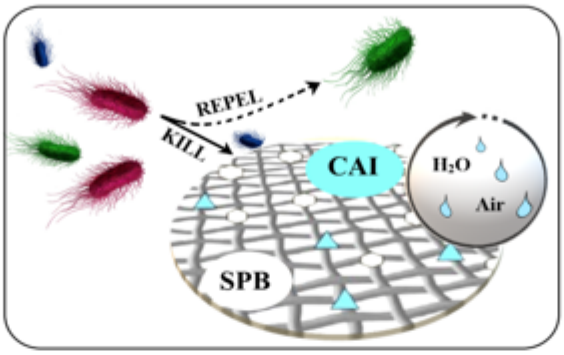

Figure 6. Cotton textiles treated with SPB / CAI, with bactericidal and antifungal activity based on the synergistic mechanism of "repel-kill" effect

By employing the surface modification, the antibacterial and antifungal properties can be bestowed for other materials used in packaging industry. Namely by depositing or incorporating agents with bactericidal and antifungal activity in the polyethylene (PE) and polypropylene (PP) films normally used in food packaging.

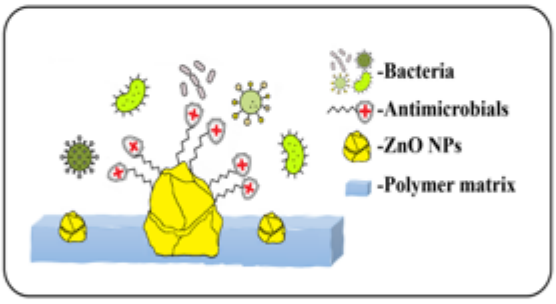

Figure 7. Modification of a PE/PP film with nanoparticles loaded with natural antimicrobials

Thus, polypropylene films can incorporate silver nanoparticles, metal oxides or silica. By loading the NPs with antibacterial agents such as essential oils (Figure 7) a synergic activity can be obtained.

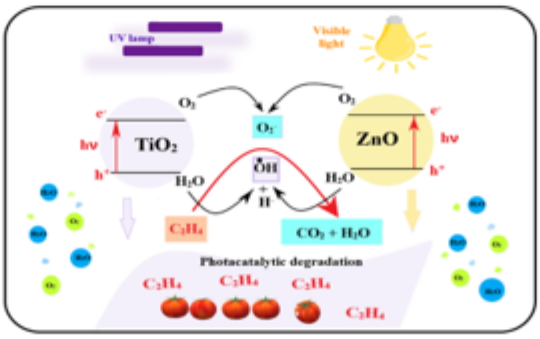

Figure 15. Diagram of CS-TiO_2 -ZnO nanocomposite activation to oxidize ethylene by exposure to UV radiation and visible light

Another type of nanoparticle embedded in chitosan films that can enhance antibacterial properties is TiO_2. Tomatoes packaged in CS-TiO_2 film underwent minor changes than those packaged in plain chitosan film or in the control sample (Figure 15). The results suggested that TiO_2 nanoparticles incorporated into the chitosan film have photocatalytic activity and degrade ethylene, delaying the post-harvest ripening process [97].

1.4. Toxicity considerations

Most of the biopolymers used for the innovative antibacterial and antifungal packaging are considered safe for human use as they are also biocompatible, and some of them are edible as FDA labels them as GRAS. Among them cellulose, alginate or chitosan in micron scale are considered GRAS for example. Large quantities of above mentioned polymers can present some adverse effects. For example, cellulose can affect the microbial flora of the digestive system and can diminish the absorption of the nutrients [113-115].

By their interaction with the membrane's cell the nanoparticles can block the biofilm growth, but they can also be transferred to the food and be inserted into the human body where will interact with our cells [116-119]. Some toxicity of nanoparticles for various organisms and environmental concerns are already expressed in some literature reports [120-122].

Some plant extracts and certainly a large variety of essential oils have a great antioxidant activity and can even be used as antimicrobials [32-34, 164]. No toxicity is reported by literature in case of essential oils, if the amount is that found in packaging [165-167]. The only identified problem is that along with the inhibition of the pathogenic bacteria, some of beneficial flora from the digestive system might be influenced [168] but is hard to see how the packaging film can be ingested alone to maintain such concentration.

In the case of citronella (lemongrass) essential oil (CEO), the major components along with other constituents, are citronellol, citronellal and citral [35, 169]. The FDA is considering CEO as a biopesticide, essentially non-toxic [36], with a powerful antibacterial and antifungal actions [37, 170, 171].

1.5. Conclusions

In conclusion, the diminish of the food loss can be accomplished by a number of strategies. As the general public is putting pressure, the regulatory authorities act toward the acceptance of the antibacterial food packaging. As we are faced also with the ecological problem generated by the use of plastics, the main focus falls on implementation of new packaging made from biodegradable polymers. In this way both issues can be addressed, elimination of plastic pollution and obtaining antimicrobial packaging. The main polymers that are in the research objective are those that fulfill some criteria like abundant in nature, cheap and non-toxic. However, the future of the antibacterial and antifungal biodegradable packaging materials will be decided by the consumer pressure and by the legislation. Biodegradable, cheap packaging films can become the new norm that will bring us the benefits of better quality and safer food.

II. ORIGINAL CONTRIBUTIONS

Chapter 2. Materials and Methods

2.1 Materials used for the synthesis of ZnO

Solid, 99.9% pure, Zn $(Ac)_2 \cdot 2H_2O$ was purchased from Merck. The butanol 99.9% was obtained from Sigma and used as received. The synthesis of zinc oxide nanoparticles was made by forced solvolysis.

Shortly, 4.3900 g Zn $(Ac)_2 \cdot 2H_2O$ were solved in 100 mL butanol and kept at 105ºC under continuous stirring. The obtained precipitate, after 12 h, was allowed to rest and then washed, and centrifuged thrice. The resulting white nanopowder kept in the oven at t 100-105°C.

2.2 Materials used for the synthesis of Ag NPs

$AgNO_3$, polyvinylpyrrolidone (PVP), and sodium salt of the citric acid were purchased from Merck. AgNPs were synthetized by Turkevich method.

Shortly, a solution of 0.01 g $AgNO_3$ and 500 mL H_2O was obtained and kept at 70-75°C under magnetic stirring. On top of this solution, we added dropwise a solution containing 0.30g sodium salt of the citric acid which was the reduction agent.

Another solution containing 0.1g PVP was added dropwise after 40 min. In the end, a yellow solution was obtained, which contained silver nanoparticles in a concentration ~100ppm. This solution required no further purification.

2.3 Materials used for fabrication of antimicrobial alginate/chitosan films

Sodium alginate (CAS 9005-38-3) was purchased from Fisher Scientific U.K. Ltd. (Redox Lab Supplies, Bucharest, Romania). Chitosan (CAS 9012-76-4), phosphate-buffered saline (PBS), sodium salt of the citric acid, glycerin, agar and nutrient broth were purchased from Redox. The citronella (lemongrass) essential oil (EO) was obtained from Carl Roth.

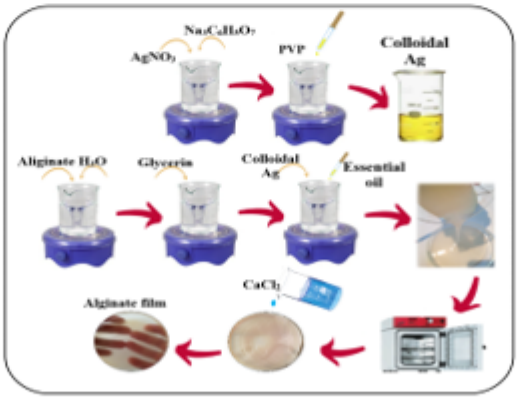

Figure 18. The obtaining of alginate/Ag/CEO packaging films

Zinc oxide nanoparticles were suspended in 15 mL H_2O, and afterwards combined with 1mL EO. This mix was undergone sonication 0.5h then added to the polymeric blend for the packaging film.

1 mL EO was added to various volumes of AgNPs solution and the mix was sonicated for 30 min before being used for the packaging films.

Solvent casting method was used for the chitosan based coatings. Typically, the combined ratio was 0.33g chitosan to 50mL acetic acid solution 1% (v/v) and 1mL of glycerine. The zinc oxide suspension or silver nanoparticles solution was added to this mix under strong stirring.

Casting method was used to obtain the alginate-base packaging. 1.5g sodium alginate salt was mixed 24h with 50mL H_2O and in the solution obtained 1mL glycerine was added. To this mix we added dropwise the silver nanoparticles/EO emulsion, under strong stirring.

A Petri type dish was used for the casting of the films. Each one was kept at 40°C for 24h. Dried films were submerged in 100mL calcium chloride 2% solution for ten minutes. At the end, the polymeric films were dried and stored at 60% RH and 20°C in closed PE bags.

2.4 Characterization techniques of synthesized materials

The materials obtained from the syntheses were characterized using appropriate techniques, being presented below:

I. Spectrophotometry -UV-Vis

A Able&Jasco spectrofotometer V560 type with solid sample accesory (integrating sphere) was used to record UV-Vis spectra. The measurement was performed in the range of 200-850 nm, with a scan speed of 200nm/min.

II. Fluorescence spectrometry

The fluorescence spectra were obtained with a Perkin/Elmer LS55 fluorimeter, in the 350-600 nm range, with a cut-off filter of 350nm and a recording speed of 200nm/min. A wavelength of 320nm from a Xe lamp was used for excitation.

III. Fourier Transform Infrared Spectroscopy (FTIR)

The investigation by the FTIR method of the obtained powders implied the prelevation of small amounts of sample using the Nicolet iS50R model spectrometer. The records were made at ambient conditions, using the ATR module (attenuated total reflection), being performed 32 scans of the samples between 4000 and 400cm^{-1}, at a resolution of 4cm^{-1}. Data retrieval and processing was performed using the Omnic work program.

IV. FTIR microscopy

FTIR maps were recorded using a Nicolet iN10-MX microscope. This is a device with a DTGS detector that provides information with a high sensitivity in the range of 4000-100 cm^{-1} and an ATR unit with diamond crystal. The spectra were recorded in iS 50 ATR mode in the range of 400-4000 cm^{-1}, with a resolution of 4 cm^{-1} by summing 32 scans to improve the quality of the spectra. Data retrieval and processing was performed using the Omnic software.

V. Scanning electron microscopy (SEM)

In this paper, scanning electron microscopy was used in order to highlight aspects related to the morphology of the synthesized samples, respectively the particle size. The acquisition of micrographs was done with the help of a high-resolution scanning electron microscope, Inspect F50, at 30KeV, for various magnifications.

VI. Energy Dispersive X-ray Spectroscopy (EDS)

The X-ray scattering spectra characteristic of the different materials proposed in the experimental activity were obtained by using a high-resolution transmission electron microscope model Tecnai G2 F30 S-TWIN, respectively a high-resolution scanning electron microscope, Inspect F50, both equipped with EDS detector.

VII. Transmission electron microscopy (TEM)

Obtaining TEM images for morpho-structural characterization was possible by using an electron microscope by high-resolution transmission model Tecnai G2 F30 S-TWIN equipped with SAED, produced by FEI, used at a voltage of 300 kV and having the point resolution and that of line of 2 Å, respectively 1 Å.

VIII. X-ray diffraction (XRD)

X-ray diffraction analyzes were performed using PAN alytical Empyrean equipment in Bragg-Brentano geometry equipped with X-ray tube with Cu anode K_α line ($\lambda_{K\alpha}$ = 1.54Å) with inline focusing, divergent slot programmable on the incident side and anti-crack programmable spreader mounted on the PIXcel3D detector on the diffracted side. Diffractograms were acquired in the range of 2θ angles 10-80° with an acquisition step of 0.2° and an acquisition time per step of 1 s. XRD analysis was performed to characterize the synthesized materials in terms of their crystallinity, as well as to identify the component phases.

IX. Thermal analysis

Thermal analysis (TG / DSC) was performed using Netzsch STA 449 C Jupiter equipment, in the temperature range 20-900 ºC, with a heating rate of 10 K/min, in dynamic air atmosphere (50 mL/ min), in open alumina crucible.

X. Biological activity

The obtained films were also characterized from a microbiological point of view, an important aspect if they are intended for human consumption. Both the films obtained, and the ingredients were tested on various types of microorganisms, both Gram-positive and Gram-negative bacteria and fungi. For testing the antimicrobial activity, strains from the Microbiology Laboratory, of the Faculty of Biology, from the University of Bucharest were used.

XI. Water vapor permeability - WVP

WVP values were obtained by using a 25mm radius permeation cups sealed by the polymeric films. Each cup contained 0.01kg of dry calcium chloride. A close box kept at 75% RH and 25°C was used to store the cups. At fixed time intervals of 8 h the cups were weighted.

Chapter 3. Goals of the thesis and originality

Protecting the food from environmental factors like moisture, dust, oxygen or microorganisms that can contaminate it during commercial chain, is the principal role of the packaging materials. Along the distribution chain, the packaging film must maintain the safety and quality of the food. Polymers used in food industry should be inert, cheap and easy to recycle.

Zinc oxide is one of the few zinc compounds recognized as safe (GRAS) by the US Food and Drug Administration. Its synthesis is reported in the literature by various methods, such as thermal decomposition [172], spray pyrolysis [173], solvothermal reactions [174], forced hydrolysis [175], sol-gel or CVD method [176]. ZnO has many applications in various fields,

such as drug delivery [177, 178], cosmetics [179], has mild astringent and antibacterial properties, and is therefore used as a topical agent in eczema and mild excoriation in wounds and for hemorrhoids [180].

Zinc oxide is a well-known antibacterial action, with multiple pathways of expressing it. There is some evidence that the antibacterial activity of ZnO is size and light dependent, but the literature available data are contradictory as to which strains are more susceptible: Gram-positive or Gram-negative. The presence of light also indicates that photocatalytic activity may be involved in promoting antibacterial activity [153]. During light activation, ZnO nanoparticles are producing reactive oxygen species (ROS) that are responsible for photocatalytic activity but also for oxidative stress, that damages the bacterial membrane.

One of the most potent antibacterial and antifungal agents is represented by the silver nanoparticles (AgNPs) [38, 181, 182]. More than 600 microorganisms (bacterial, viral and fungal strains) are affected by AgNPs according to literature reports [183-185]. The principal elements that influence the antimicrobial action of AgNPs are the size and shape, as the smaller nanoparticles, triangular shaped, are proved more active [38].

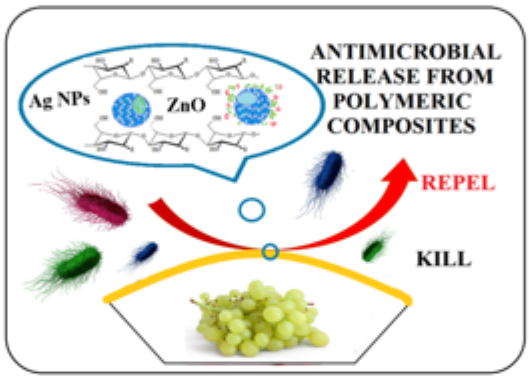

Figure 19. The combined activity of the antimicrobial package

In last years, natural extracts like essential oils have been proven to exhibit antibacterial, antifungal and antioxidant activities, some acting even as repellants for insects [32, 186-188]. Citronella essential oil (lemongrass) –CEO- has a strong antimicrobial activity and FDA consider it a bio-pesticide [36]. Geraniol, citronellol and citronellal are the principal constituents [35]. Being hydrophobic in nature, the addition of the CEO to the polymeric blend will decrease the WVP improving the packaging performance [42-44].

We used two or three antimicrobial agents, zinc oxide or/and silver nanoparticles and CEO, as a way to improve the overall antimicrobial activity of the packaging, while using small quantities of such additives.

Solvent casting method was used to obtain the chitosan films. 0.66 g chitosan were solved in 100 mL acetic acid solution (1 %*v/v*) which was mixed with 2 mL of glycerin. After chitosan solubilization a suspension of zinc oxide or/and silver nanoparticles with citronella oil was added under strong stirring in ratios from Table 2. After casting solutions in Petri dishes they were put in oven at 40 ºC for 24 h for drying. The films were stored in PE bags at 60 %RH and 20 ºC.

The zinc oxide and silver nanoparticles concentrations for the CZA series were chosen such way that two separate series could be formed. In each one of them, a type of nanoparticle

was kept with a constant concentration and the other type of nanoparticle was variable. The combinations of nanoparticles and the citronella oil was chose by surveying the literature reports and synergic activity [189, 190]. As such, the zinc oxide amount increased in the series CZA1-3, while the silver nanoparticles amount was kept constant. The other way around, the zinc oxide was kept constant and silver amount was increased in the series CZA4, CZA2, and CZA5. For each sample, the citronella oil quantity was the same, 1 mL.

Table 2. The chitosan–nanoparticles–citronella essential oil (CEO) films composition.

Sample Code	Chitosan (g in 100 mL of 1% (*v/v*) Acetic Acid)	ZnO NPs (g in 15 mL Water)	Ag NPs (mL Solution)	CEO (mL)
CZ1	0.66	0.165	0	1
CZ2	0.66	0.33	0	1
CZ3	0.66	0.66	0	1
CZ4	0.66	0.99	0	1
CA1	0.66	-	10	1
CA2	0.66	-	15	1
CA3	0.66	-	20	1
CA4	0.66	-	30	1
CZA1	0.66	0.33	15	1
CZA2	0.66	0.66	15	1
CZA3	0.66	0.99	15	1
CZA4	0.66	0.66	10	1
CZA5	0.66	0.66	30	1

By same casting method were prepared also the alginate films with the amounts from the table 3. Zinc oxide nanoparticles were suspended in 10 mL H_2O and after mixing 1 mL citronella oil the solution was sonicated. The suspension was added to a solution obtained from 3 g sodium alginate in 100 mL H_2O and magnetically stirred for one day. As plasticizer 2 mL glycerin were added.

Table 3. The alginate–ZnO NPs–citronella essential oil (CEO) films composition.

Sample Code	Alginate (g in 100 mL Water)	ZnO NPs (g in 15 mL Water)	Glycerol (mL Solution)	CEO (mL)
A	3.00	0.00	2	0
AZ1	3.00	0.05	2	1
AZ2	3.00	0.10	2	1
AZ3	3.00	0.25	2	1
AZ4	3.00	0.50	2	1

Similar, were obtained the alginate films with Ag NPs (Table 4). A certain amount of solution containing Ag NPs was mixed with 1 mL CEO and was sonicated further for 15 min before being used to prepare AAg1–AAg4. 3 g alginate was added to a beaker of 100 mL water and left to dissolve for 24 h under stirring.

Afterwards, 2 mL of glycerol was added to the alginate solution. A previously prepared emulsion of Ag NPs and CEO was added to the alginate solution, under vigorous stirring.

Table 4. The alginate–Ag NPs– citronella essential oil (CEO) films composition.

Sample Code	Alginate (g in 100 mL water)	Ag NPs (mL of 100 ppm Solution)	Glycerol (mL Solution)	CEO (mL)
A	3.00	0	2	0
AAg1	3.00	5.0	2	1.0
AAg2	3.00	10.0	2	1.0
AAg3	3.00	25.0	2	1.0
AAg4	3.00	50.0	2	1.0

Each solution was put in a Petri dish and was left to dry in an oven for 24 h at 40 °C. A control film without nanoparticles and CEO was prepared in the same way. After film drying, 200 mL $CaCl_2$ solution (0.2 M) was added to each Petri-dish and the films were left submerged for 5 min. The films were removed from the Petri-dish and were stored in zip lock plastic bags at 20 °C and 60% relative humidity (RH).

Chapter 4. Literature Review and Articles

4.1 Antibacterial biodegradable films based on alginate with silver nanoparticles and lemongrass essential oil – innovative packaging for cheese

nanomaterials MDPI

Article

Antibacterial Biodegradable Films Based on Alginate with Silver Nanoparticles and Lemongrass Essential Oil–Innovative Packaging for Cheese

Ludmila Motelica [1], Denisa Ficai [1], Ovidiu-Cristian Oprea [1,*], Anton Ficai [1,2], Vladimir-Lucian Ene [1], Bogdan-Stefan Vasile [1], Ecaterina Andronescu [1,2] and Alina-Maria Holban [1,3]

[1] Faculty of Applied Chemistry and Material Science, University Politehnica of Bucharest, 060042 Bucharest, Romania; motelica_ludmila@yahoo.com (L.M.); denisa.ficai@upb.ro (D.F.); anton.ficai@upb.ro (A.F.); vladimir.lene@gmail.com (V.-L.E.); vasile_bogdan_stefan@yahoo.com (B.-S.V.); ecaterina.andronescu@upb.ro (E.A.); alina.m.holban@bio.unibuc.ro (A.-M.H.)
[2] Academy of Romanian Scientists, 050045 Bucharest, Romania
[3] Microbiology & Immunology Department, Faculty of Biology, University of Bucharest, 077206 Bucharest, Romania
* Correspondence: ovidiu.oprea@upb.ro or ovidiu73@yahoo.com; Tel.: +40-214-023-986

Abstract: Replacing the petroleum-based materials in the food industry is one of the main objectives of the scientists and decision makers worldwide. Biodegradable packaging will help diminish the environmental impact of human activity. Improving such biodegradable packaging materials by adding antimicrobial activity will not only extend the shelf life of foodstuff, but will also eliminate some health hazards associated with food borne diseases, and by diminishing the food spoilage will decrease the food waste. The objective of this research was to obtain innovative antibacterial films based on a biodegradable polymer, namely alginate. Films were characterized by environmental scanning electron microscopy (ESEM), Fourier-transform infrared spectroscopy (FTIR) and microscopy, complex thermal analysis (TG-DSC-FTIR), UV-Vis and fluorescence spectroscopy. Water vapor permeability and swelling behavior were also determined. As antimicrobial agents, we used silver spherical nanoparticles (Ag NPs) and lemongrass essential oil (LGO), which were found to act in a synergic way. The obtained films exhibited strong antibacterial activity against tested strains, two Gram-positive (*Bacillus cereus* and *Staphylococcus aureus*) and two Gram-negative (*Escherichia coli* and *Salmonella* Typhi). Best results were obtained against *Bacillus cereus*. The tests indicate that the antimicrobial films can be used as packaging, preserving the color, surface texture, and softness of cheese for 14 days. At the same time, the color of the films changed (darkened) as a function of temperature and light presence, a feature that can be used to monitor the storage conditions for sensitive food.

Keywords: biodegradable; alginate film; antibacterial packaging; lemongrass essential oil; silver nanoparticles; edible packaging; cheese; time-temperature indicator (TTI)

Citation: Motelica, L.; Ficai, D.; Oprea, O.-C.; Ficai, A.; Ene, V.-L.; Vasile, B.-S.; Andronescu, E.; Holban, A.-M. Antibacterial Biodegradable Films Based on Alginate with Silver Nanoparticles and Lemongrass Essential Oil–Innovative Packaging for Cheese. *Nanomaterials* **2021**, *11*, 2377. https://doi.org/10.3390/nano11092377

Academic Editor: Sabbatini Luigia

Received: 15 August 2021
Accepted: 8 September 2021
Published: 13 September 2021

Publisher's Note: MDPI stays neutral with regard to jurisdictional claims in published maps and institutional affiliations.

1. Introduction

The majority of food packaging materials used at present are based on petrochemical products or cellulose, due to historical factors such as low cost or mechanical and barrier properties [1,2]. The pressure of environmental concerns will phase out the petroleum-based materials, which will increase the need for innovative, biodegradable polymeric packaging materials such as chitosan [3], alginate [4], cellulose [5], starch [6], pullulan [7], polylactic acid [8], etc. The need to decrease the food waste, and the desire to increase the food safety and to prolong the shelf life creates pressure on the food packaging industry to develop and adopt new antimicrobial materials [9–11]. Besides chitosan, none of these biopolymers present antimicrobial activity [12]. Therefore, various antimicrobial agents have to be mixed with the polymeric matrix to obtain the desired antibacterial or antifungal

activities [13]. Such innovative antimicrobial biodegradable materials can diminish the microorganisms' proliferation and thus will reduce the food spoilage, increase the shelf life, and help provide a better food quality [14–18].

Sodium alginate (A) belongs to the polysaccharides class, being the salt of alginic acid [19]. Usually, the source of alginate is the marine algae brown seaweed, which makes it acceptable for people with religious dietary restrictions [20]. Alginate is one of the most versatile polymers, being used in various applications from drug delivery systems [21], to environmental depollution [22], wound healing, and tissue engineering [23]. Alginate is considered GRAS (generally recognized as safe) by the US Food and Drug Administration, therefore is a natural choice for packaging materials [24,25]. It is water-soluble and can be easy functionalized [26]. Mechanical properties are enhanced by adding plasticizers, glycerol being the most common choice due to its superior compatibility with the polymeric matrix [27,28]. Antibacterial activity can be bestowed to the alginate by adding various nanoparticles such as ZnO [29], Ag [30], CuO [31], natural extracts [32–34], or other substances of pharmaceutical interest [35–37].

Silver nanoparticles (Ag NPs) are one of the most potent antimicrobial agents [38–40]. The literature reports at least 650 microorganisms, including viruses, along with bacteria and fungi, affected by Ag NPs [41–43]. The shape and size of Ag NPs are the main factors that influence the antimicrobial activity, the smaller, triangular nanoparticles being more potent [39].

Essential oils and other natural plant extracts present a huge potential as antioxidants, antimicrobials, and even as insect repellants [44–47]. Lemongrass essential oil (LGO) is considered a bio-pesticide in the US [48]. The major constituents are citronellal, geraniol, and citronellol [49]. As a hydrophobic extract, the LGO addition to the alginate film will also improve the water vapor permeability (WVP) performance of the polymeric matrix [50–52].

For the LGO, there is no reported toxicity at concentrations used, but concerns are expressed about the impact on beneficial gut microbiota [53,54]. The introduction of nanomaterials such as Ag NPs into food packaging presents some potential drawbacks, beside advantages such as antimicrobial activity or improved UV-barrier properties. It is mandatory to study the toxicity related to the use of metallic nanoparticles. One way to minimize the impact is to decrease the concentration level of Ag NPs in the packaging films. By combining Ag NPs antimicrobial activity with that of LGO, we demonstrate that very low concentrations of metallic nanoparticles can be used, while still maintaining a strong antibacterial activity.

The objective of this research was to obtain a biodegradable, antibacterial material that can be used as packaging for soft cheese (usually with a shelf life of 4 days at 4–8 °C). The literature presents a couple of alginate-base films, with Ag NPs, used as packaging for meat [55,56] or vegetables [57], but none for cheese. In addition, to the best of our knowledge, here we report for the first time the obtaining of the alginate–Ag NPs–LGO system. We used two antimicrobials, Ag NPs and LGO, in order to enhance the final antibacterial activity of films, while introducing smaller amounts of antibacterial agents. The films were characterized from physico-chemical point of view, and the antibacterial activity was determined against two Gram-positive (*Bacillus cereus* and *Staphylococcus aureus*) and two Gram-negative (*Escherichia coli* and *Salmonella* Typhi) bacterial strains. The performed antibacterial test indicates that, while the film with the highest Ag NPs concentration exhibited the best antibacterial activity, the rest of films, with lower concentrations of Ag NPs, were still performing very well against tested bacterial strains. Therefore, combining the antimicrobial agents can be a successful strategy to decrease the amount of used substances, which limits their potential toxic activity against human organism.

2. Materials and Methods

2.1. Materials

Silver nitrate, polyvinylpyrrolidone (PVP), and sodium citrate were obtained from Merck. Sodium alginate (CAS 9005-38-3) was purchased from Fisher Scientific U.K. Ltd. (Redox Lab Supplies, Bucharest, Romania). Phosphate-buffered saline (PBS), sodium citrate, glycerol, nutrient broth, and agar were obtained from Sigma Aldrich (Redox Lab Supplies, Bucharest, Romania). Lemongrass essential oil (LGO) was purchased from Carl Roth (Amex-Lab, Bucharest, Romania). All the chemicals were used without any further purification.

The soft telemea cheese (S.C. Fabrica de lapte Brasov S.A., Halchiu, BV, Romania) was obtained from a local supermarket in Bucharest, Romania.

2.2. Synthesis of Silver Nanoparticles

AgNPs were synthetized as described in [58]. Briefly, 0.02 g $AgNO_3$ was dissolved in 100 mL water under vigorous stirring at 70 °C. Then, 20 mL solution of 0.35 g sodium citrate was added dropwise as a reduction agent. After 30 min, a third solution (0.1 g PVP in 5 mL) was added dropwise. The yellow solution containing AgNPs (100 ppm) was used without further purifications.

2.3. Synthesis of Alginate/Ag/LGO Films

A certain amount of solution containing Ag NPs was mixed with 1 mL LGO and was sonicated further for 15 min before being used to prepare AAg1–AAg4 films (Table 1).

Table 1. The alginate–Ag NPs–lemongrass essential oil (LGO) films composition.

Sample Code	Alginate (g in 100 mL Water)	Ag NPs (mL of 100 ppm Solution)	Glycerol (mL Solution)	LGO (mL)
A	3.00	0	2	0
AAg1	3.00	5.0	2	1.0
AAg2	3.00	10.0	2	1.0
AAg3	3.00	25.0	2	1.0
AAg4	3.00	50.0	2	1.0

Alginate films were obtained by casting method. Shortly, 3 g alginate was added to a beaker of 100 mL water and left to dissolve for 24 h under stirring. Afterwards, 2 mL of glycerol was added to the alginate solution. A previously prepared emulsion of Ag NPs and LGO was added to the alginate solution, under vigorous stirring.

Each solution was put in a Petri dish and was left to dry in an oven for 24 h at 40 °C. A control film without Ag NPs and LGO was prepared in the same way. After drying, 200 mL $CaCl_2$ solution (2%) was added to each Petri dish, and the films were left submerged for 10 min. Finally, the films were removed from the Petri dish and were stored in zip lock plastic bags at 20 °C and 60% relative humidity (RH) (Figure S1).

2.4. Characterization of Alginate Films

In order to investigate the films surface morphology and microstructure, scanning electron micrographs were obtained using an environmental scanning electron microscope VERSA 3D (ESEM, Thermo-Fisher, former FEI Company, Eindhoven, The Netherlands).

Bright Field and High Resolution a Transmission Electron Microscopy (BF-TEM, HR-TEM) images coupled with Selected Area Electron Diffraction (SAED) pattern were recorded using High-Resolution 80-200 TITAN THEMIS transmission microscope FEI (Thermo Fisher Scientific, Waltham, MA, USA).

Fourier transform infrared spectra were recorded with a Nicolet iS50 FTIR spectrometer (Thermo Fisher Scientific Inc., Waltham, MA, USA).

FTIR 2D maps were recorded with a Nicolet iS50R FTIR microscope (Thermo Fisher Scientific Inc., Waltham, MA, USA).

A Perkin Elmer (Waltham, MA, USA) LS55 spectrometer was used to measure the photoluminescence spectrum (PL).

A JASCO V560 spectrophotometer (JASCO Inc., Easton, PA, USA) was used to measure the UV–Vis spectra. The opacity values were calculated as $A_{600}/x = -\log T_{600}/x$, where A_{600} is the absorbance at 600 nm, T_{600} is the fractional transmittance at 600 nm and x is the film thickness in mm. A higher opacity value indicates that the film is less transparent [59].

Thermal analysis, TG-DSC (thermogravimetry and differential scanning calorimetry), was performed with a STA 449C F3 apparatus, from Netzsch (Selb, Germany). The evolved gases were analyzed with a FTIR Tensor 27 from Bruker (Bruker Co., Ettlingen, Germany), equipped with a thermostated gas cell.

For the determination of water vapor permeability (WVP), we used permeation cups with a diameter of 30 mm, sealed with a sample film, as described in [60]. In each cup we placed 1 g of dried $CaCl_2$. The permeation cups were placed in a container at a temperature of 25 °C and 100% relative humidity. Their weight was measured at fix intervals (8 h) for four days.

The swelling capacity was determined as described in [61]. Shortly, square samples of ~3 × 3 cm were cut from the fresh films and were dried in a desiccator for 48 h. Once dried, the samples were weighed (0.2 mg) (W_0), then placed in 200 mL water or phosphate buffer saline (PBS) to allow swelling. The samples were first weighed at 15 min intervals, then each 30 min for three hours, and finally at 24 h intervals for the next days as the maximum swelling capacities were attained. The Equation (1) formula for degree of swelling (D) was used to calculate the swelling ratio:

$$D = (W_t - W_0)/W_0 \quad (1)$$

The antibacterial activity was evaluated against two model Gram-positive (*Bacillus cereus* ATCC 13061 and *Staphylococcus aureus* ATCC 25923) and two Gram-negative (*Escherichia coli* ATCC 25922 and *Salmonella enterica* Typhi ATCC 14023) bacteria, which are relevant in food bacterial contamination. The strains were maintained as glycerol stocks at −80 °C. All experiments were designed and performed in triplicate.

To qualitatively screen the antibacterial effect of the obtained materials, we utilized an adapted diffusion assay, respecting the general rules exposed in the CLSI 2020 and in our recent study [62].

Cheese samples (~cubic shape with size of 2–3 cm) were packed in alginate and AAg1–AAg4 films and placed in a refrigerator (4 °C ± 1 °C and 75% R.H.) for 14 days. Samples were weighed again after 14 days for the mass loss test. Weight loss was monitored by measuring the mass change of each sample, and was calculated as percentage lost from the initial mass. The pH was measured initially and after 14 days.

The results were statistically evaluated using the analysis of variance (ANOVA) performed with Microsoft Excel 2016 (Microsoft Corp., Redmond, WA, USA), having installed the XLSTAT 2020.5.1 add-on. The Shapiro–Wilk test was used to check the normal distribution of the data; we assessed the homoscedasticity of the residuals by Levene's test; and the results were compared by Tukey's (HSD) test so that the pairs of films that differed in terms of statistical significance were revealed ($p < 0.05$).

More details about specific conditions for each analysis are presented in the Supplementary Materials.

3. Results and Discussion

The samples were characterized by transmission electron microscopy (TEM) and scanning electron microscopy (SEM), Fourier Transform Infrared (FTIR) spectroscopy and microscopy, UV-Vis and fluorescence spectroscopy, and thermal analysis TG-DSC. Water vapor permeability (WVP) and swelling behavior were also determined.

3.1. Transmision Electron Microscopy

The BF-TEM image presented in Figure 1 presents particles existing in the Ag NPs 100 ppm solution. They are round shaped, with a diameter of approximately 5 to 25 nm, having a bimodal distribution. The Ag NPs are highly crystalline, with bigger ones composed of 2–3 crystallites. Therefore, the large nanoparticles can be considered polycrystalline, while the smaller ones are monocrystalline. Similar distribution was reported before, for both laboratory synthesized and commercially available [63,64]. Most probably during grain formation, before adding the capping agent, some crystallites become agglomerate, thus larger nanoparticles grow along smaller ones.

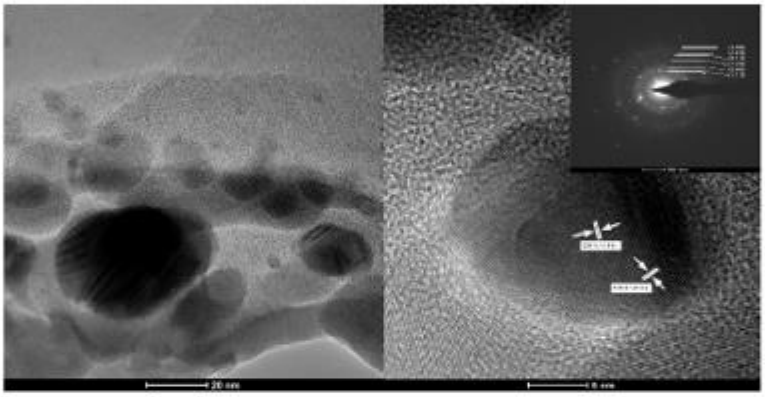

Figure 1. The TEM images for the obtained Ag NPs. Selected area electron diffraction (SAED) pattern in the inset.

The identified Miller indices in HR-TEM are the (111) corresponding to 2.36 Å distance. From SAED pattern, the only phase identified is that of FCC (face-centered cubic) silver, corresponding to the standard data JCPDS File No. 04-0783.

3.2. Environmental Scanning Electron Microscopy

According to the pressure–humidity–temperature diagram of the liquid–vapor phase equilibrium for water, the expected pressure in the working chamber at a temperature of 0.5 °C and humidity of ~8% is estimated at ~50 Pa [65]. Thus, the analysis chamber was prepared by performing vacuum purge cycles, between pressures of 30–150 Pa, to avoid contamination of samples with impurities from the atmosphere. In order to capture the microstructure of the specimen, without the detrimental interference of high-vacuum and high-voltage, the image acquisitions are made in low vacuum conditions (50 Pa), a temperature of 0.5 °C, a relative humidity of ~8%, at a beam voltage of 2 kV, with a working distance of about 8.3 mm. The surface of the films is presented in Figure 2.

The ESEM images show that with the increasing content of Ag from AAg1 to AAg4, the surface of the alginate films does not change in either morphology nor pore size distribution. The only noticeable difference resides in the fact that Ag aggregates are more disperse in the specimens that contain a higher amount of nanoparticles, without significantly affecting their size. This observation leads to the idea that during the nucleation and crystal growth of silver nanoparticles, the PVP surfactant is limiting the crystal growth and stabilizing the aggregate size. The alginate polymer in which the Ag NPs were dispersed does not contribute towards further noteworthy agglomeration of nanoparticles due to sterically stabilization of Ag NPs from the synthesis stage [66].

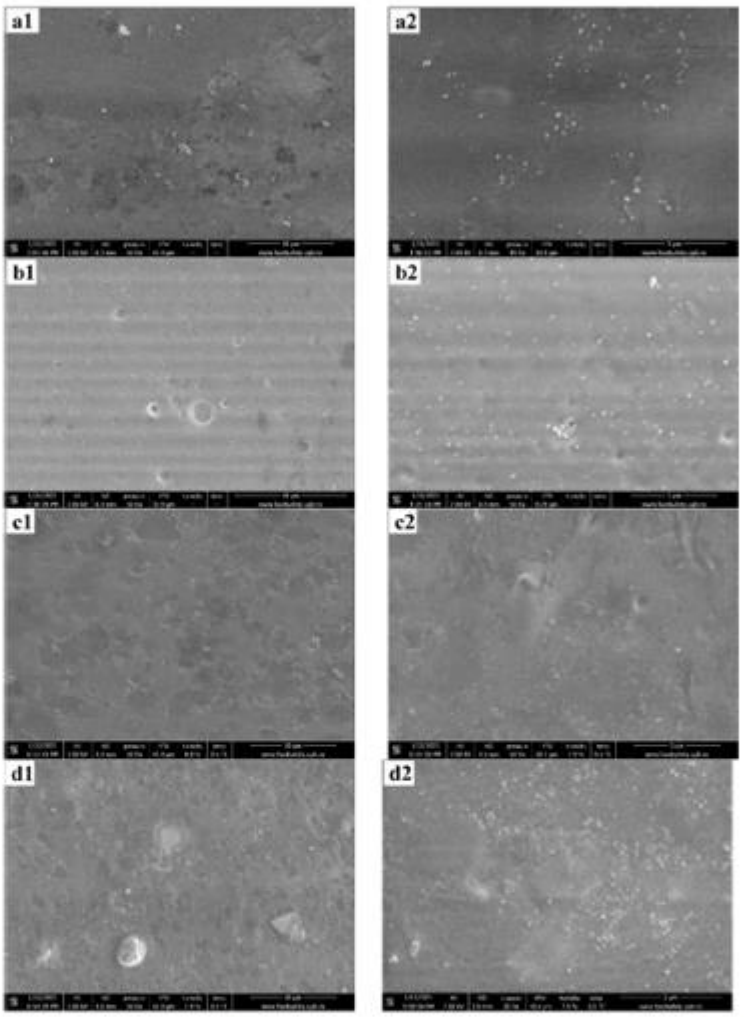

Figure 2. The ESEM micrographs for AAg1 (**a1**,**a2**); AAg2 (**b1**,**b2**); AAg3 (**c1**,**c2**); and AAg4 (**d1**,**d2**) films.

More insightful information was extracted from a film fracture, presented in Figure 3. The interior of the polymeric film shows spherical micropores of variable sizes. Most probably, their formation is related to the presence of LGO microdroplets dispersion into the alginate matrix. Moreover, inside the polymer pores, Ag NPs agglomerates are found at the surface, suggesting that there is a positioning preference of the agglomerates at the pore-material interface, rather than a homogenous distribution of the latter throughout the material volume.

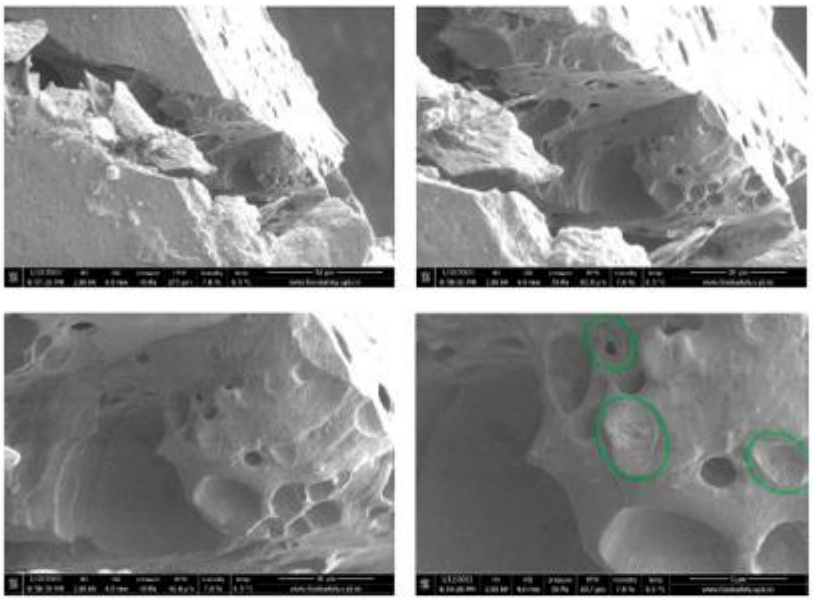

Figure 3. The near-fracture micrographs of AAg4 film. Ag NPs agglomerates inside potes.

The presence of such micropores will most probably have an impact on mechanical and barrier properties of the films. Although the extent at which the overall mechanical and barrier properties of the film are affected by the preferred positioning of Ag NPs agglomerates on the pore-material interface is questionable, pores themselves act as points of minimal resistance for the film.

3.3. *FTIR Spectroscopy and Microscopy*

3.3.1. FTIR Spectroscopy

The effects induced by the Ag NPs and LGO addition to the alginate matrix were investigated by FTIR spectroscopy. The peaks corresponding to the main absorption peaks and the associated vibration modes are presented in Table 2. The broad band from the 3270–3287 cm^{-1} corresponds to the presence of -O-H moiety from alginate and moisture as well.

Table 2. Assignment of relevant IR absorption bands of alginate (A) and AAg1–AAg4 films.

Sample/Assignment	A	AAg1	AAg2	AAg3	AAg4
υ_{as}C-O-C	1031	1028	1027	1026	1027
υ_{s}COO^{-}	1416	1408	1407	1409	1410
υ_{as}COO^{-}	1596	1602	1600	1602	1604
C = O group of LGO [67]		1740	1738	1738	1739
υC-H (sat)	2921	2930	2925	2921	2921
υO-H	3278	3277	3270	3284	3287

The intense 2921–2930 cm^{-1} peaks are attributed to the C_{sp3}-H symmetric vibrations of the alginate, while small 3075 cm^{-1} peak belongs to C_{sp2}-H symmetric vibration from LGO components. The 1027–1031 cm^{-1} peaks were attributed to the glycosidic bond in the polysaccharide chain. The observed small shifts could indicate interactions between

alginate negative charged -COO⁻ groups and uncoated zones of Ag NPs surface or the interaction of Ag NPs with -C = O moiety of the pyrrolidone cycle from the PVP coating [68].

3.3.2. FTIR Microscopy

With the help of FTIR microscopy, we looked at spatial distribution of Ag NPs and LGO into the alginate matrix. The maps corresponding to the 1740 cm^{-1} and 1030 cm^{-1} are presented for the AAg1–AAg4 films in Figure 4, together with the microscopic view of the analyzed region.

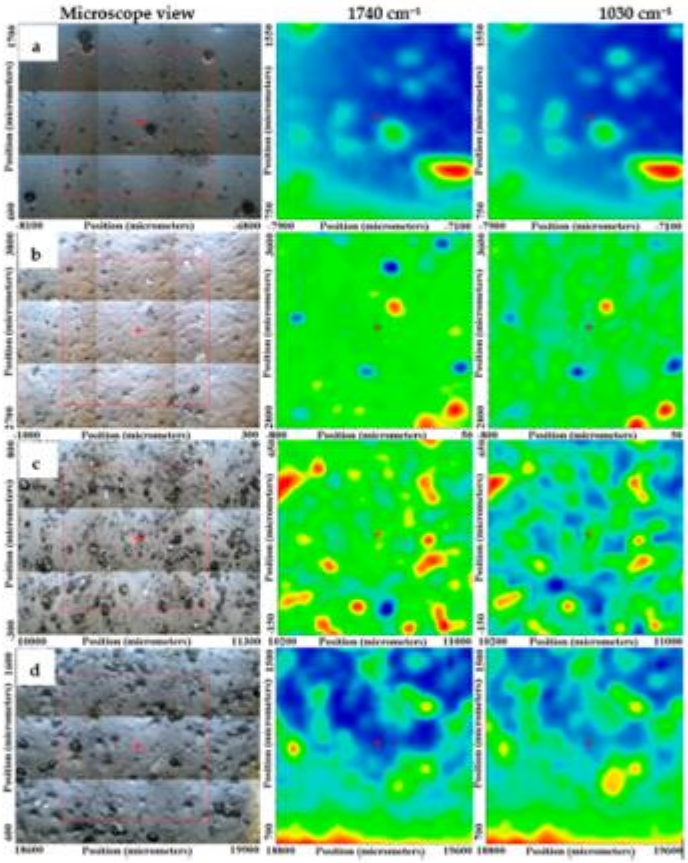

Figure 4. FTIR maps for the AAg1 (**a**); AAg2 (**b**); AAg3 (**c**); and AAg4 (**d**) films.

The FTIR maps at those two wavenumbers for AAg1 and AAg2 are quite similar, indicating a uniform distribution of the components in the analyzed area. The increase in Ag NPs quantity in AAg3 and AAg4 films generated some local accumulations, clusters, or defects such as pores, which induce a less homogeneous structure for these two samples, at a level of tens of μm, maximum. Nevertheless, even for these two samples, the FTIR maps are not so different, therefore the samples can be considered as having a good homogeneity.

3.4. UV-Vis and Fluorescence Spectroscopy

UV-Vis Spectroscopy

The UV-Vis spectroscopy is widely used for the Ag NPs characterization and synthesis monitoring as it is sensible to the presence of nanoparticles and gives information about their morphology and size uniformity. The absorption peak generated by the localized surface plasmon resonance is the main characteristic of the UV-Vis spectrum for Ag NPs [69]. It can be observed at wavelengths starting from 400 nm up to 600 nm depending on Ag NPs shape and size [70–72]. In addition, UV-Vis spectra can be used to monitor the stability of the Ag NPs suspension.

Our Ag NPs solution was proven stable over 3 months' storage, at room temperature, under dark conditions, the spectrum being virtually unchanged, with the band exhibiting the maximum absorption peak at 422 nm (Figure 5). This indicates that the Ag NPs are well capped by the PVP and do not agglomerate [73]. The peak broadness indicates that, although small, the size of nanoparticles varies, as seen also from TEM images, from 5 to 25 nm.

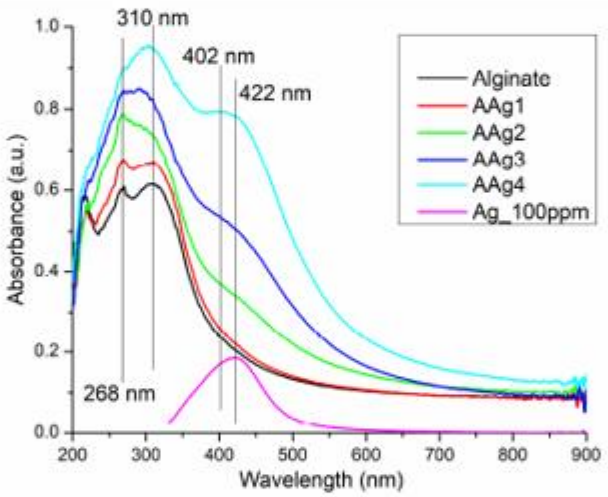

Figure 5. UV-Vis spectra for Ag NPs, alginate, and AAg1–AAg4 films.

The UV-Vis spectra for the alginate and AAg1–AAg4 films, presented in Figure 5, indicates the existence of a darkening effect in correlation with the increase in Ag NPs content. The AAg1 film has a marginally higher absorbance in UV region and is virtually identical with alginate film in the visible domain. For the AAg2–AAg4, the increased absorbance can be observed in the violet-blue region, which starts as a shoulder in the AAg2 sample, and develops into a separate broad band with the peak at 402 nm for AAg4. The presence of the 402 nm band can be assigned to the increasing concentration of Ag NPs (ten times higher in AAg4 than in AAg1).

The UV absorbance is also increasing with the Ag NPs content. Both UV and Vis light barriers are important features for food packaging, as a high absorbance will protect the critical nutrients (vitamins, lipids, or proteins) from photo-oxidation reactions promoted by high-energy photons. Different superscripts (a, b) in the last column are significantly different ($p < 0.05$). Values are given as the mean ± SD from triplicate determination.

The incorporation of Ag NPs into the alginate film is increasing the opacity, but only marginally (Table 3), from 0.48 ± 0.02 to a maximum of 0.67 ± 0.04, and therefore the alginate films can be considered transparent [74].

Table 3. Thickness and opacity for alginate (A) and alginate/Ag NPs/LGO (AAg1–AAg4) films.

Sample	Alginate	AAg1	AAg2	AAg3	AAg4
Thickness (mm)	0.22 ± 0.01	0.21 ± 0.02	0.27 ± 0.02	0.30 ± 0.03	0.35 ± 0.02
Opacity	0.48 ± 0.02 [a]	0.51 ± 0.05 [a]	0.54 ± 0.04 [a]	0.55 ± 0.06 [a]	0.67 ± 0.04 [b]

Different superscript letters indicate statistically significant differences between films ($p < 0.05$).

The AAg1–AAg4 films can become less transparent over time, depending on the storage conditions, e.g., temperature or light presence. As expected, a higher Ag NPs content will promote a large absorbance change (Figure 6a). Temperature change (4 °C vs. 30 °C) will also increase the absorbance change, but the presence of light has the highest impact on the film darkening (Figure 6b). The main reason for the changing of color is the oxidation of Ag NPs [75]. As the reaction rate will increase with the temperature, the samples stored at 30 °C will darken quicker than those stored at 4 °C. Similar reports are found in the literature [76,77]. This indicates that such films can be used as a time-temperature indicator (TTI) for storage conditions of food. Cumulative higher temperature and light (which for shelf food translate into exposure time) lead to a change of transparency, and therefore can indicate the freshness of packed food.

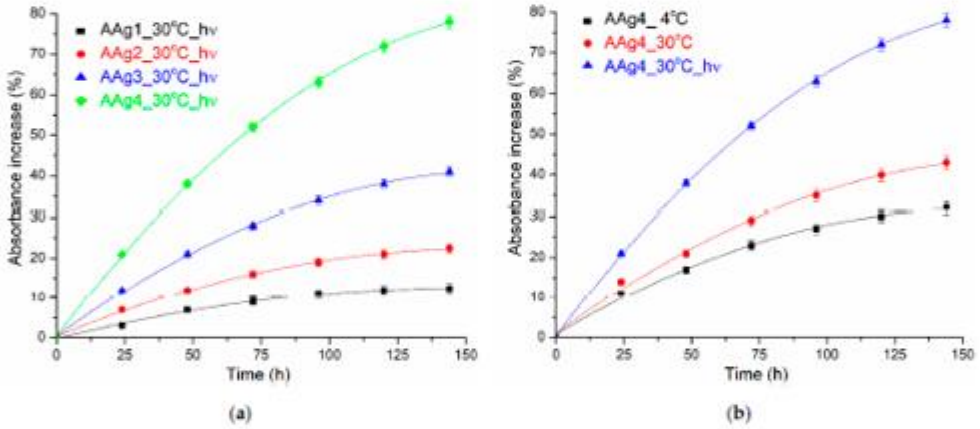

Figure 6. Color darkening (absorbance increase at 402 nm) for AAg1–AAg4 films: as function of Ag NPs content (**a**) and as function of temperature and light presence (**b**).

The Ag NPs are well known for their fluorescent properties. The literature reports different emission peaks in dependence on the excitation wavelength and Ag NPs morphology [78]. Usually, it is reported that the surface plasmon extinction peak is around 400 nm, while the fluorescent emissions at higher wavelengths are attributed to ultra-small Ag NPs (~5 nm) [79]. Here, we report Ag NPs that present the surface plasmon extinction peak at 368 nm, with a second emission band at 446 nm (Figure 7a). Surface plasmon related emission peaks under 400 nm have been reported in the previous literature, e.g., 384 nm [80], 375 nm [81], or 330 nm [78]. The broad visible emission band from 446 nm can be attributed to $sp \rightarrow d$ radiative transitions due to Ag–Ag interactions. Similar shaped spectra, with surface plasmon emission placed in UV region accompanied by a broad visible emission peak in blue region are reported [78,82].

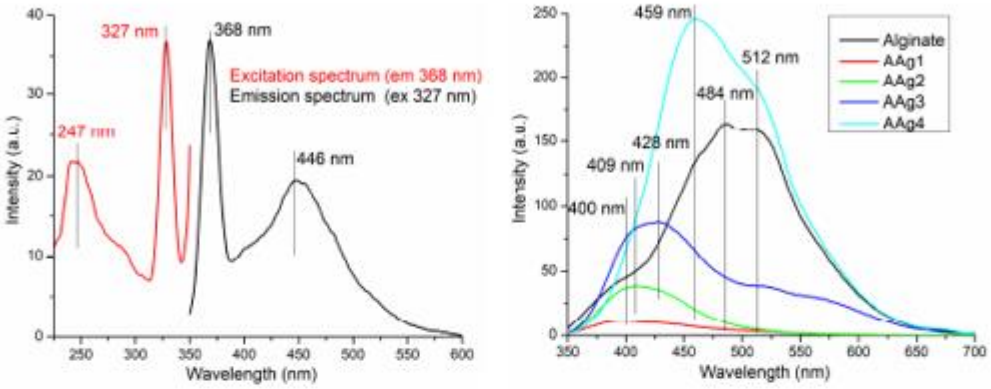

Figure 7. The fluorescence spectra for Ag NPs (**a**) alginate and AAg1–AAg4 films (**b**).

The fluorescence spectra for the alginate and AAg1–AAg4 films presented in Figure 7b, indicates the existence of Ag NPs–alginate interactions. The addition of a small quantity of Ag NPs in AAg1 sample leads to an emission band centered on 400 nm, much weaker than those corresponding to the Ag NPs or alginate. The interactions between Ag NPs and alginate polymeric chains are probably responsible for blocking the surface plasmon emission, but also for quenching the alginate fluorescence. Increasing the Ag NPs content of the composite films is generating a stronger and broader visible emission band, while the peaks are red-shifted towards 459 nm, with a shoulder at 512 nm.

This can be attributed to the existence of local Ag NPs agglomerations (as seen in ESEM images), which promotes Ag–Ag interactions, either directly or mediated by moieties of alginate. A similar effect of nanoparticles on alginate fluorescence was reported in [4].

3.5. *Thermal Analysis TG/DSC–FTIR*

The thermal analysis of alginate and AAg1–AAg4 samples indicates that the composite films have a lower thermal stability than the simple alginate one, the mass loss starting at low temperatures, i.e., under 100 °C (Figure 8).

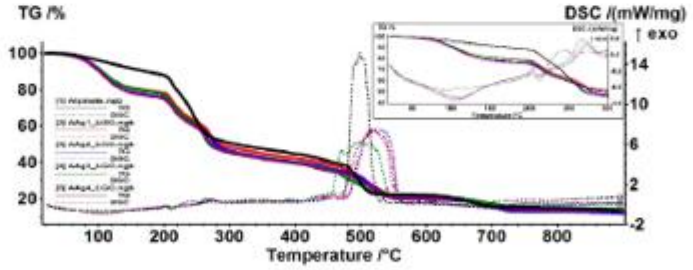

Figure 8. TG/DSC curves for alginate and AAg1–AAg4 films.

The alginate film starts losing mass at about 70 °C, most probably water, the process being accompanied on DSC curve by a weak endothermic effect with minimum at 93.2 °C. Up to 200 °C the sample is losing 12.14% of its initial mass.

The samples AAg1–AAg4 present a larger mass loss up to 200 °C (22–25%), the corresponding endothermic effect being more intense and shifted towards higher temperatures (105–110 °C). This can be attributed to the elimination of various volatile compounds belonging to LGO incorporated into the alginate films, which means that approximatively 10% of the sample mass is consisting of LGO. The hypothesis is sustained by the FTIR analysis of evolved gases. Figure 9, FTIR 3D plot vs. T (°C), reveals at low temperatures the presence of absorption bands around 3000 cm^{-1} which are attributed to C-H vibration in various hydrocarbons, which can be attributed to elimination of LGO volatile components (Figure 9).

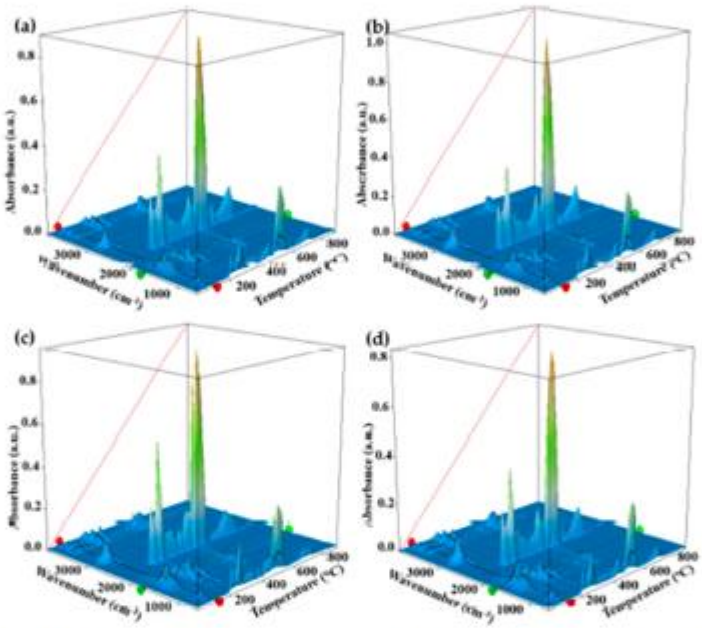

Figure 9. The 3D FTIR plot of evolved gases for AAg1 (**a**); AAg2 (**b**); AAg3 (**c**); and AAg4 (**d**).

The oxidation process of alginate matrix starts after 200 °C, when multiple exothermic effects, with low intensity, can be observed on DSC curve (inset of Figure 8). The FTIR profile for the absorption band from 2355 cm^{-1}, corresponding to CO_2 elimination from sample (Figure 9), presents multiple peaks after 200 °C. Each peak corresponds to an oxidation process, the most intense being attributed to the burning of residual carbonaceous mass around 500 °C.

3.6. *Water Vapor Permeability (WVP)*

The barrier properties of alginate films are very important, as they must prevent the loss of flavor, water, or other volatile substances from the packed food [83]. The water vapor permeability (WVP) values best describe the moisture capacity to migrate between environment and food, through the packaging film. Microbial spoilage can be related to good moisture permeability. Therefore, it is important to determine the values for WVP (Table 4).

Table 4. Water vapor permeability for simple alginate and AAg1–AAg4 films.

Film Code	WVP (10^{-10} g/Pa·m·s)
A	5.718 ± 0.011^{a}
AAg1	2.753 ± 0.042^{b}
AAg2	2.706 ± 0.035^{b}
AAg3	2.696 ± 0.024^{b}
AAg4	2.691 ± 0.054^{b}

Different superscript letters indicate statistically significant differences between films ($p < 0.05$).

The simple alginate film presented an average value for WVP when compared to similar reports [30,83]. The higher value can be explained by the glycerol addition, which generates hydrogen bonds with alginate and therefore increases the inter-chains distance, allowing moisture to penetrate easier [84].

Smaller values for WVP are obtained for the AAg1–AAg4 films, but they are not statistically different among them. This can indicate that the main cause for this decrease is the presence of LGO rather than the addition of Ag NPs. The clear hydrophobic nature of LGO generates micron and sub-micron drops inside the alginate films.

As thermal analysis data indicates, a large proportion of LGO is trapped inside the polymeric matrix (~10% *w*/*w*).

As such, the water molecules pathway becomes longer and obstructed by hydrophobic zones represented by LGO [85], which act as physical barriers [13,83] (Figure 10).

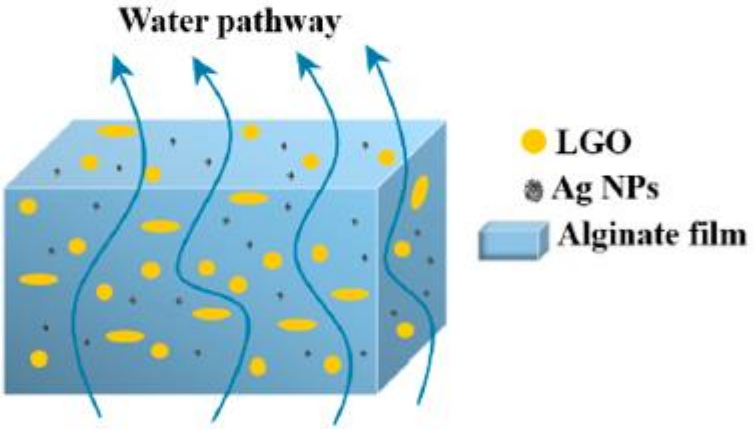

Figure 10. The proposed mechanism behind decrease in WVP values for AAg1–AAg4 films.

3.7. Swelling Study

The swelling behavior was assessed in PBS (pH = 7.4) and in distilled water. An increase in the swelling capacity with the increase in Ag NPs content can be observed in both cases (Table 5).

As the Ag NPs amount increased, the AAg1–Aag4 films have a higher capacity of water uptake. This increasing capacity can be related to the pores' dimensions at the microscopic level, and with the space between alginate chains at molecular level. The Ag NPs are stabilized with PVP. The presence of more silver nanoparticles and PVP can induce a wider gap between alginate chains, and therefore a higher water retention capacity. The pores can act as traps for water molecules. A higher pore density therefore can trap a larger water quantity (e.g., for AAg4 film).

Table 5. Swelling capacity (as mass increase in %) for the alginate and AAg1–AAg4 films.

Sample	Water / PBS					
	0.25 h	0.5 h	1 h	2 h	3 h	24 h
A	42.54% / 81.99%	61.22% / 182.05%	86.14% / 374.36%	101.83% / 595.63%	104.69% / 659.28%	102.76% / 741.75%
AAg1	61.12% / 113.94%	84.92% / 276.24%	103.67% / 451.33%	108.38% / 556.02%	105.53% / 596.58%	100.43% / 564.89%
AAg2	82.97% / 167.42%	95.59% / 347.91%	108.65% / 489.04%	114.35% / 589.77%	119.33% / 623.66%	121.06% / 704.31%
AAg3	110.13% / 231.88%	123.90% / 454.65%	130.79% / 580.89%	126.41% / 647.52%	128.91% / 691.74%	128.53% / 675.24%
AAg4	136.47% / 295.55%	151.97% / 549.36%	162.99% / 696.36%	167.90% / 719.23%	169.77% / 837.85%	168.81% / 799.79%

In water, the films were swelling close to maximum capacity in 2 h, with more than half of the water quantity being retained in first 15 min. The swelling increased slowly up to 3 h, further measurements indicating a weight stabilization (the measurement at 24 h is presented in Table 5, but the films were stable for 30 days).

The swelling study in PBS produced larger values for water retention capacity (up to six times higher than those obtained for water study).

This can be explained by the slow replacement of Ca^{2+} ions with Na^{+} ones, which leads to the destruction of the Ca-alginate "egg-box" structure. This leads to an increasing gap between polymeric chains and, as such, larger amounts of water can be retained. As the replacement of Ca^{2+} ions proceeds, the resulting sodium alginate will start to dissolve, therefore the sample will start to lose mass. At 72 h the films are completely disintegrated in PBS solution.

3.8. Antibacterial Activity

The results obtained for the AAg1–AAg4 films against four relevant food born infections bacterial strains, two Gram-positive (*S. aureus; B. cereus*) and two Gram-negative (*S.* Typhi; *E. coli*), indicate a strong antibacterial activity (Figure 11).

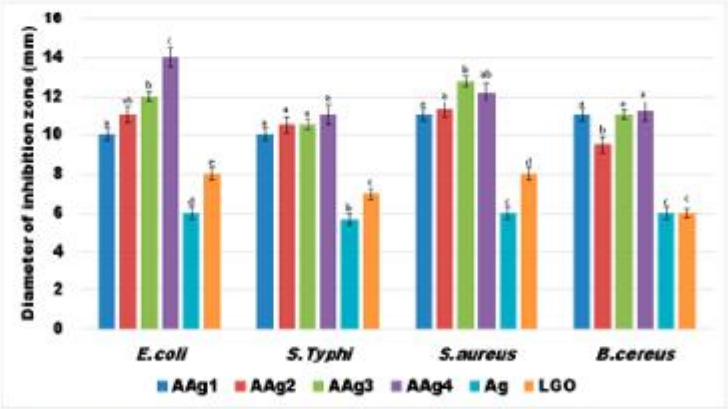

Figure 11. Measured growth inhibition diameters (mm) for the evaluated bacterial strains in the presence of AAg1–AAg4 films. Different small letters indicate statistically significant differences between films ($p < 0.05$).

This suggests a large spectrum of antibacterial activity for the alginate films that contains both Ag NPs and LGO. As the simple alginate film exhibited no antibacterial activity, it is safe to assume that the strong antibacterial effect of AAg1–AAg4 films comes from Ag NPs combined with substances from the essential oil.

The results obtained suggest that growth inhibition is dependent of Ag NPs concentration in case of *E. coli* and *S. aureus*, the largest inhibition zones being observed for AAg3 and AAg4 samples, followed by AAg2 and AAg1 (Figure 11). In the case of *S.* Typhi and *B. cereus* the diameter of inhibition zone does not differ significantly among AAg1–AAg4 samples, but it has a consistently constant high value. This indicates that both Ag NPs and LGO act synergically, conferring a strong antibacterial activity.

LGO alone has a lower antibacterial effect, but in combination with Ag NPs the values for growth inhibition diameters are higher. The Ag NPs solution also presented a modest, constant value for the growth inhibition zone among all four tested strains. Therefore, the high values obtained for the antibacterial activity of AAg1–AAg4 suggest the existence of synergism between Ag NPs and LGO. The probable mechanism is related to the LGO changing the adenosine triphosphate concentration and hyperpolarization of the cell wall, and decreasing of the cytoplasmic pH [86,87], which in turn makes it easier for the silver ions released by the Ag NPs to damage the membrane and bind the proteins and enzymes [88], disrupting vital processes inside the cell.

Strong planktonic growth inhibition was observed in cases of *E. coli* and *B. cereus* (for AAg2–AAg4 films especially) indicating that the antibacterial compounds from LGO and Ag NPs could be released from the alginate polymeric matrix and affect the evolution of free bacterial cells (Figure 12). In cases of *S.* Typhi and *S. aureus* strains, the development of individual cells was also inhibited mostly by AAg3–AAg4 samples, suggesting a susceptibility to the presence of larger amounts of Ag NPs.

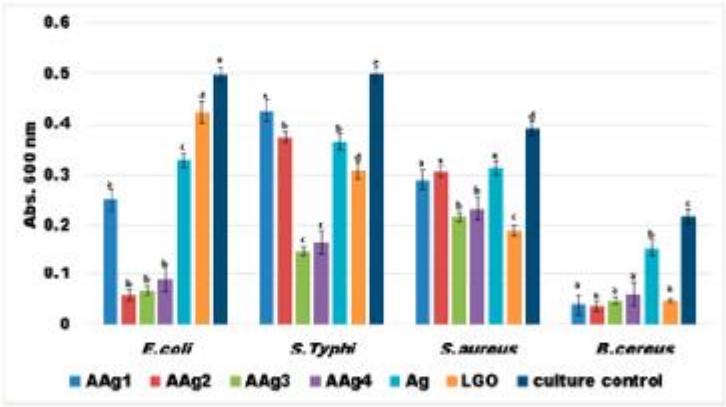

Figure 12. Absorbances at 600 nm indicating growth of planktonic cultures in the presence of AAg1–AAg4 films for 24 h at 37 °C. Different small letters indicate statistically significant differences between films ($p < 0.05$).

Similar results were also obtained for the bacterial biofilm development and its attachment in the presence of AAg1–AAg4 films (Figure 13). The obtained data indicate that biofilm development is significantly reduced in the cases of *E. coli* and *B. cereus*. The *B. cereus* was again the most susceptible strain, as we saw in the case of planktonic growth. In the case of *E. coli* and *S. aureus*, a clear dependence of Ag NPs is evidenced, consistent with the results from growth inhibition diameter measurements.

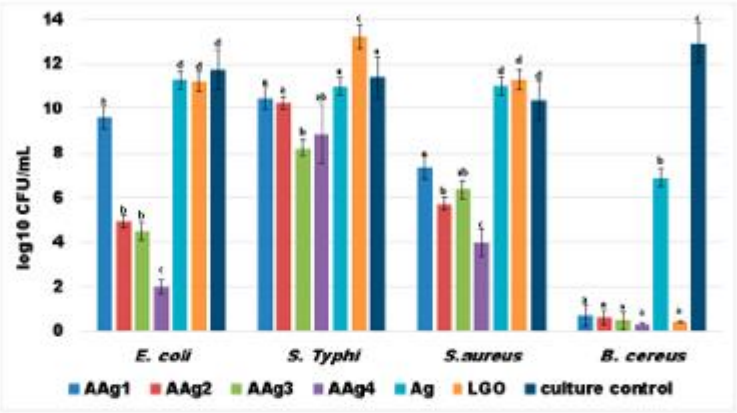

Figure 13. Values of $\log_{10}$CFU/mL for the tested bacterial strains, expressing biofilm embedded cells developed on control and AAg1–AAg4 films after 24h incubation. Different small letters indicate statistically significant differences between films ($p < 0.05$).

Biofilm growth inhibition results, presented in Figure 13, indicate that the films are highly efficient towards Gram-positive *B. cereus* strain. A good antibacterial activity can also be observed for the other strains, especially for AAg4 sample. The samples with higher Ag NPs content exhibited best antibacterial activity, so we can state that biofilm growth inhibition is dependent of Ag NPs concentration. The results suggest that these films can be tailored to combat specific pathogens, depending on the desired application and susceptibility of microbial strains.

The literature indicates that Ag NPs present a stronger antibacterial activity against *S. aureus* than *E. coli* [89,90]. For the LGO, as well as the antifungal activity, a strong antibacterial activity against Gram-positive bacterial strains such as *B. cereus* is reported [16,91].

Our study has revealed that combining the two antibacterial agents, Ag NPs and LGO, a strong synergic antibacterial activity is obtained. The AAg1–AAg4 films are efficient against both types of pathogens, Gram-positive and Gram-negative, despite the former being usually more resistant due to its complex cellular wall [91,92].

3.9. Evaluation of Potential Use of AAg1–AAg4 Films as Food Packaging

Cheese is an important food made from casein, fat, and water. When it is not salted, uncontrolled and extensive development of microorganisms is contributing to cheese's short shelf life. Different cheese varieties need some bacterial cultures to be produced, and this creates an infection hazard from the cheese-borne species such as *Escherichia coli*, *Salmonella enterica*, or *Staphylococcus aureus* [4]. Samples of soft cheese of approximatively 10.00–13.00 g were weighed and packed in alginate or AAg1–Aag4 films. The samples were stored for 14 days at 4 °C ± 1 °C and 75% RH. After 14 days, the samples were visually checked, weighed, and the pH was measured. The cheese bits appearances (Figure 14), mass loss (Table 6), and pH data suggest that AAg1–AAg4 films can preserve cheese for up to 2 weeks.

The obtained results indicate that the cheese samples stored in AAg1–AAg4 films were better preserved comparatively with the control sample. The white, soft texture was maintained for samples packed in AAg1–AAg4 films, while the control sample changed its color and became harder. The control sample turned dark yellow due to spoilage microorganisms' growth. The sample packed in AAg1 film also presented some minor spoilage coloration on the edge, but the samples packed in AAg2–AAg4 films retained the

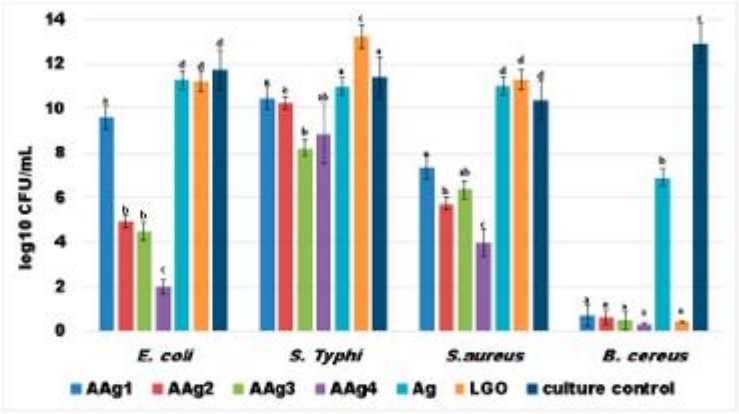

Figure 13. Values of $\log_{10}$CFU/mL for the tested bacterial strains, expressing biofilm embedded cells developed on control and AAg1–AAg4 films after 24h incubation. Different small letters indicate statistically significant differences between films ($p < 0.05$).

Biofilm growth inhibition results, presented in Figure 13, indicate that the films are highly efficient towards Gram-positive *B. cereus* strain. A good antibacterial activity can also be observed for the other strains, especially for AAg4 sample. The samples with higher Ag NPs content exhibited best antibacterial activity, so we can state that biofilm growth inhibition is dependent of Ag NPs concentration. The results suggest that these films can be tailored to combat specific pathogens, depending on the desired application and susceptibility of microbial strains.

The literature indicates that Ag NPs present a stronger antibacterial activity against *S. aureus* than *E. coli* [89,90]. For the LGO, as well as the antifungal activity, a strong antibacterial activity against Gram-positive bacterial strains such as *B. cereus* is reported [16,91].

Our study has revealed that combining the two antibacterial agents, Ag NPs and LGO, a strong synergic antibacterial activity is obtained. The AAg1–AAg4 films are efficient against both types of pathogens, Gram-positive and Gram-negative, despite the former being usually more resistant due to its complex cellular wall [91,92].

3.9. Evaluation of Potential Use of AAg1–AAg4 Films as Food Packaging

Cheese is an important food made from casein, fat, and water. When it is not salted, uncontrolled and extensive development of microorganisms is contributing to cheese's short shelf life. Different cheese varieties need some bacterial cultures to be produced, and this creates an infection hazard from the cheese-borne species such as *Escherichia coli*, *Salmonella enterica*, or *Staphylococcus aureus* [4]. Samples of soft cheese of approximatively 10.00–13.00 g were weighed and packed in alginate or AAg1–Aag4 films. The samples were stored for 14 days at 4 °C ± 1 °C and 75% RH. After 14 days, the samples were visually checked, weighed, and the pH was measured. The cheese bits appearances (Figure 14), mass loss (Table 6), and pH data suggest that AAg1–AAg4 films can preserve cheese for up to 2 weeks.

The obtained results indicate that the cheese samples stored in AAg1–AAg4 films were better preserved comparatively with the control sample. The white, soft texture was maintained for samples packed in AAg1–AAg4 films, while the control sample changed its color and became harder. The control sample turned dark yellow due to spoilage microorganisms' growth. The sample packed in AAg1 film also presented some minor spoilage coloration on the edge, but the samples packed in AAg2–AAg4 films retained the

initial aspect, color, surface texture, and softness. This indicates that these antimicrobial films are capable of preserving the soft cheese and extending the shelf life.

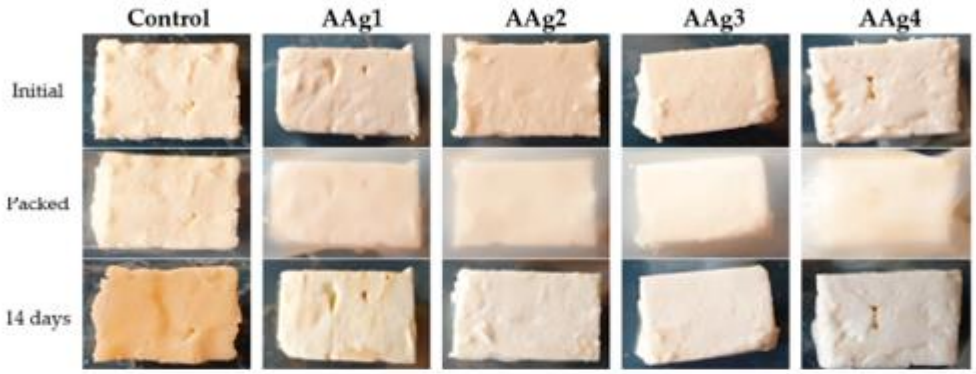

Figure 14. Visual appearance of soft cheese bits packaged in alginate control film and AAg1–AAg4 films, initial and after 14 days storage at 4 °C and 75% relative humidity.

Table 6. Weight loss for cheese bits coated with alginate control and AAg1–AAg4 films during storage.

Sample/ Weight Loss (%)	A	AAg1	AAg2	AAg3	AAg4
14 days	39.32 ± 0.51^{a}	2.39 ± 0.21^{b}	2.31 ± 0.17^{b}	2.61 ± 0.26^{b}	2.55 ± 0.24^{b}

Different superscript letters in the same column indicate statistically significant differences between films ($p < 0.05$).

The weight of the cheese samples was measured at the start and after 14 days of storage (Table 6). The samples packed in AAg1–AAg4 films presented a small mass loss, around 2.50% value, while the control sample lost 39.32%. This can be explained by the better barrier properties of the composite films, as seen in Section 3.6. The cheese eliminates water vapors, and with less hindrance from the simple alginate film, they are lost in surrounding environment.

Modification of the pH value for the cheese can indicate the presence of spoilage microorganisms. Therefore, the pH value was measured initially and after 14 days. For the samples packed in AAg1–AAg4 films, the value remained constant at 4.5. Similar constant values are reported in the literature when spoilage is absent [93]. For the control sample, the pH value dropped to 4.3, most probably due to growth and fermentation activity of microorganisms.

Nevertheless, a full study on the migration magnitude of Ag NPs to the food surface to assess the possible toxic effects is mandatory.

4. Conclusions

Novel innovative biodegradable alginate films were obtained and characterized. A strong antibacterial activity was conferred by the addition of Ag NPs and lemongrass essential oil. The antimicrobial agents are shown to act in a synergic fashion, the AAg1–AAg4 samples presenting a large antibacterial activity spectrum, against both Gram-positive and Gram-negative strains, best results being obtained against *B. cereus*. The antibacterial films were tested as packaging for soft cheese, the preliminary test indicating a good capacity to preserve it up to 14 days. The light and water barrier properties of the alginate films were enhanced by the addition of LGO and Ag NPs. The films are transparent, but at 30 °C and in the presence of light they tend to darken, with the

absorbance increasing by up to 78% compared with those stored at 4 °C in the absence of light, where the absorbance increased only with max 32%, in a six day interval. This process can be used to monitor the storage conditions for sensitive food.

Supplementary Materials: The following are available online at https://www.mdpi.com/xxx/s1, Materials and Methods. Figure S1: Preparation scheme for the alginate films with Ag NPs and LGO. Figure S2: XRD of obtained Ag NPs (JCPDS 04-0783) (a) and of AAg4 film (b). Figure S3: TG / DSC curves for alginate (a); AAg1 (b); AAg2 (c); AAg3 (d) and AAg4 (e) films.

Author Contributions: Conceptualization, D.F., A.F. and L.M.; methodology, L.M. and O.-C.O.; formal analysis, V.-L.E., A.-M.H., B.-S.V. and A.F.; investigation, V.-L.E., A.-M.H., B.-S.V. and D.F.; resources, E.A.; data curation, L.M.; writing—original draft preparation, L.M. and O.-C.O.; writing—review and editing, A.F.; supervision, D.F.; project administration, E.A.; and funding acquisition, O.-C.O. All authors have read and agreed to the published version of the manuscript.

Funding: This work was supported by a grant of the Romanian Ministry of Research and Innovation, CCCDI—UEFISCDI, project number PN-III-P1-1.2-PCCDI-2017-0689/P1. "Lib2Life—Revitalizarea bibliotecilor și a patrimoniului cultural prin tehnologii avansate" within PNCDI III. The APC was funded by University POLITEHNICA of Bucharest.

Data Availability Statement: The data is included in the main text and/or the supplementary materials.

Conflicts of Interest: The authors declare no conflict of interest. The funders had no role in the design of the study; in the collection, analyses, or interpretation of data; in the writing of the manuscript, or in the decision to publish the results.

References

1. Motelica, L.; Ficai, D.; Ficai, A.; Oprea, O.C.; Kaya, D.A.; Andronescu, E. Biodegradable Antimicrobial Food Packaging: Trends and Perspectives. *Foods* **2020**, *9*, 1438. [CrossRef]
2. Motelica, L.; Ficai, D.; Oprea, O.C.; Ficai, A.; Andronescu, E. Smart Food Packaging Designed by Nanotechnological and Drug Delivery Approaches. *Coatings* **2020**, *10*, 806. [CrossRef]
3. Radulescu, M.; Ficai, D.; Oprea, O.; Ficai, A.; Andronescu, E.; Holban, A.M. Antimicrobial Chitosan based Formulations with Impact on Different Biomedical Applications. *Curr. Pharm. Biotechnol.* **2015**, *16*, 128–136. [CrossRef]
4. Motelica, L.; Ficai, D.; Oprea, O.C.; Ficai, A.; Trusca, R.D.; Andronescu, E.; Holban, A. Biodegradable Alginate Films with ZnO Nanoparticles and Citronella Essential Oil—A Novel Antimicrobial Structure. *Pharmaceutics* **2021**, *13*, 1020. [CrossRef] [PubMed]
5. Lemnaru, G.-M.; Trusca, R.D.; Ilie, C.-I.; Tiplea, R.D.; Ficai, D.; Oprea, O.; Stoica-Guzun, A.; Ficai, A.; Ditu, L.-M. Antibacterial Activity of Bacterial Cellulose Loaded with Bacitracin and Amoxicillin: In Vitro Studies. *Molecules* **2020**, *25*, 4069. [CrossRef] [PubMed]
6. Wilpiszewska, K.; Antosik, A.K.; Schmidt, B.; Janik, J.; Rokicka, J. Hydrophilic Films Based on Carboxymethylated Derivatives of Starch and Cellulose. *Polymers* **2020**, *12*, 2447. [CrossRef]
7. Li, S.B.; Yi, J.J.; Yu, X.M.; Wang, Z.Y.; Wang, L. Preparation and characterization of pullulan derivative/chitosan composite film for potential antimicrobial applications. *Int. J. Biol. Macromol.* **2020**, *148*, 258–264. [CrossRef] [PubMed]
8. Conte, A.; Longano, D.; Costa, C.; Ditaranto, N.; Ancona, A.; Cioffi, N.; Scrocco, C.; Sabbatini, L.; Conto, F.; Del Nobile, M.A. A novel preservation technique applied to fiordilatte cheese. *Innov. Food Sci. Emerg. Technol.* **2013**, *19*, 158–165. [CrossRef]
9. Gherasim, O.; Popescu, R.C.; Grumezescu, V.; Mogoșanu, G.D.; Mogoanta, L.; Iordache, F.; Holban, A.M.; Vasile, B.S.; Birca, A.C.; Oprea, O.C.; et al. MAPLE Coatings Embedded with Essential Oil-Conjugated Magnetite for Anti-Biofilm Applications. *Materials* **2021**, *14*, 1612. [CrossRef]
10. Dimulescu, I.A.; Nechifor, A.C.; Bardaca, C.; Oprea, O.; Pascu, D.; Totu, E.E.; Albu, P.C.; Nechifor, G.; Bungau, S.G. Accessible Silver-Iron Oxide Nanoparticles as a Nanomaterial for Supported Liquid Membranes. *Nanomaterials* **2021**, *11*, 1204. [CrossRef]
11. Vasile, B.S.; Oprea, O.; Voicu, G.; Ficai, A.; Andronescu, E.; Teodorescu, A.; Holban, A. Synthesis and characterization of a novel controlled release zinc oxide/gentamicin-chitosan composite with potential applications in wounds care. *Int. J. Pharm.* **2014**, *463*, 161–169. [CrossRef]
12. Gingasu, D.; Mindru, I.; Patron, L.; Ianculescu, A.; Vasile, E.; Marinescu, G.; Preda, S.; Diamandescu, L.; Oprea, O.; Popa, M.; et al. Synthesis and Characterization of Chitosan-Coated Cobalt Ferrite Nanoparticles and Their Antimicrobial Activity. *J. Inorg. Organomet. Polym. Mater.* **2018**, *28*, 1932–1941. [CrossRef]
13. Motelica, L.; Ficai, D.; Ficai, A.; Trusca, R.D.; Ilie, C.I.; Oprea, O.C.; Andronescu, E. Innovative Antimicrobial Chitosan/ZnO/Ag NPs/Citronella Essential Oil Nanocomposite-Potential Coating for Grapes. *Foods* **2020**, *9*, 1801. [CrossRef] [PubMed]
14. Zhao, L.Y.; Duan, G.G.; Zhang, G.Y.; Yang, H.Q.; He, S.J.; Jiang, S.H. Electrospun Functional Materials toward Food Packaging Applications: A Review. *Nanomaterials* **2020**, *10*, 150. [CrossRef] [PubMed]

15. Xing, Y.G.; Li, X.L.; Guo, X.L.; Li, W.X.; Chen, J.W.; Liu, Q.; Xu, Q.L.; Wang, Q.; Yang, H.; Shui, Y.R.; et al. Effects of Different TiO(2)Nanoparticles Concentrations on the Physical and Antibacterial Activities of Chitosan-Based Coating Film. *Nanomaterials* **2020**, *10*, 1365. [CrossRef]
16. Viktorova, J.; Stupak, M.; Rehorova, K.; Dobiasova, S.; Hoang, L.; Hajslova, J.; Thanh, T.V.; Tri, L.V.; Tuan, N.V.; Ruml, T. Lemon Grass Essential Oil does not Modulate Cancer Cells Multidrug Resistance by Citral-Its Dominant and Strongly Antimicrobial Compound. *Foods* **2020**, *9*, 585. [CrossRef] [PubMed]
17. Fleancu, M.C.; Olteanu, N.L.; Rogozea, A.E.; Crisciu, A.V.; Pincovschi, I.; Mihaly, M. Physical-chemical parameters promoting phase changes in non-ionic environmental-friendly microemulsions. *Fluid Phase Equilib.* **2013**, *337*, 18–25. [CrossRef]
18. Sonseca, A.; Madani, S.; Rodriguez, G.; Hevilla, V.; Echeverria, C.; Fernandez-Garcia, M.; Munoz-Bonilla, A.; Charef, N.; Lopez, D. Multifunctional PLA Blends Containing Chitosan Mediated Silver Nanoparticles: Thermal, Mechanical, Antibacterial, and Degradation Properties. *Nanomaterials* **2020**, *10*, 22. [CrossRef]
19. Vizzini, P.; Beltrame, E.; Zanet, V.; Vidic, J.; Manzano, M. Development and Evaluation of qPCR Detection Method and Zn-MgO/Alginate Active Packaging for Controlling Listeria monocytogenes Contamination in Cold-Smoked Salmon. *Foods* **2020**, *9*, 1353. [CrossRef]
20. Kontominas, M.G. Use of Alginates as Food Packaging Materials. *Foods* **2020**, *9*, 1440. [CrossRef]
21. Chen, K.Y.; Zeng, S.Y. Preparation and Characterization of Quaternized Chitosan Coated Alginate Microspheres for Blue Dextran Delivery. *Polymers* **2017**, *9*, 210. [CrossRef]
22. Chang, Y.H.; Huang, C.F.; Hsu, W.J.; Chang, F.C. Removal of Hg^{2+} from aqueous solution using alginate gel containing chitosan. *J. Appl. Polym. Sci.* **2007**, *104*, 2896–2905. [CrossRef]
23. Paduraru, A.; Ghitulica, C.; Trusca, R.; Surdu, V.A.; Neacsu, I.A.; Holban, A.M.; Birca, A.C.; Iordache, F.; Vasile, B.S. Antimicrobial Wound Dressings as Potential Materials for Skin Tissue Regeneration. *Materials* **2019**, *12*, 1859. [CrossRef] [PubMed]
24. Gheorghita, R.; Amariei, S.; Norocel, L.; Gutt, G. New Edible Packaging Material with Function in Shelf Life Extension: Applications for the Meat and Cheese Industries. *Foods* **2020**, *9*, 562. [CrossRef]
25. Gheorghita, R.; Gutt, G.; Amariei, S. The Use of Edible Films Based on Sodium Alginate in Meat Product Packaging: An Eco-Friendly Alternative to Conventional Plastic Materials. *Coatings* **2020**, *10*, 166. [CrossRef]
26. Gago, C.; Antao, R.; Dores, C.; Guerreiro, A.; Miguel, M.G.; Faleiro, M.L.; Figueiredo, A.C.; Antunes, M.D. The Effect of Nanocoatings Enriched with Essential Oils on 'Rocha' Pear Long Storage. *Foods* **2020**, *9*, 240. [CrossRef] [PubMed]
27. Fahmy, A.; Khafagy, R.M.; Elhaes, H.; Ibrahim, M.A. Molecular properties of polyvinyl alcohol/sodium alginate composite. *Biointerface Res. Appl. Chem.* **2020**, *10*, 4734–4739.
28. Mahcene, Z.; Khelil, A.; Hasni, S.; Akman, P.K.; Bozkurt, F.; Birech, K.; Goudjil, M.B.; Tornuk, F. Development and characterization of sodium alginate based active edible films incorporated with essential oils of some medicinal plants. *Int. J. Biol. Macromol.* **2020**, *145*, 124–132. [CrossRef]
29. Fahmy, A.; Khafagy, R.M.; Elhaes, H.; Ibrahim, M.A. Molecular Modeling Analyses of Polyvinyl Alcohol/ Sodium Alginate/ZnO Composite. *Egypt. J. Chem.* **2021**, *64*, 1149–1166.
30. Lan, W.T.; Li, S.Y.; Shama, S.; Zhao, Y.Q.; Sameen, D.E.; He, L.; Liu, Y.W. Investigation of Ultrasonic Treatment on Physicochemical, Structural and Morphological Properties of Sodium Alginate/AgNPs/Apple Polyphenol Films and Its Preservation Effect on Strawberry. *Polymers* **2020**, *12*, 2096. [CrossRef]
31. Saravanakumar, K.; Sathiyaseelan, A.; Mariadoss, A.V.A.; Hu, X.W.; Wang, M.H. Physical and bioactivities of biopolymeric films incorporated with cellulose, sodium alginate and copper oxide nanoparticles for food packaging application. *Int. J. Biol. Macromol.* **2020**, *153*, 207–214. [CrossRef] [PubMed]
32. Luo, Y.; Liu, H.Q.; Yang, S.Z.; Zeng, J.R.; Wu, Z.Q. Sodium Alginate-Based Green Packaging Films Functionalized by Guava Leaf Extracts and Their Bioactivities. *Materials* **2019**, *12*, 2923. [CrossRef] [PubMed]
33. Hammoudi, N.; Cherif, H.Z.; Borsali, F.; Benmansour, K.; Meghezzi, A. Preparation of active antimicrobial and antifungal alginate-montmorillonite/lemon essential oil nanocomposite films. *Mater. Technol.* **2020**, *35*, 383–394. [CrossRef]
34. Shahbazi, Y.; Shavisi, N. Effects of sodium alginate coating containing Mentha spicata essential oil and cellulose nanoparticles on extending the shelf life of raw silver carp (*Hypophthalmichthys molitrix*) fillets. *Food Sci. Biotechnol.* **2019**, *28*, 433–440. [CrossRef] [PubMed]
35. Trapani, A.; Corbo, F.; Agrimi, G.; Ditaranto, N.; Cioffi, N.; Perna, F.; Quivelli, A.; Stefano, E.; Lunetti, P.; Muscella, A.; et al. Oxidized Alginate Dopamine Conjugate: In Vitro Characterization for Nose-to-Brain Delivery Application. *Materials* **2021**, *14*, 3495. [CrossRef]
36. Sportelli, M.C.; Longano, D.; Bonerba, E.; Tantillo, G.; Torsi, L.; Sabbatini, L.; Cioffi, N.; Ditaranto, N. Electrochemical Preparation of Synergistic Nanoantimicrobials. *Molecules* **2020**, *25*, 49. [CrossRef]
37. Tsirigotis-Maniecka, M. Alginate-, Carboxymethyl Cellulose-, and kappa-Carrageenan-Based Microparticles as Storage Vehicles for Cranberry Extract. *Molecules* **2020**, *25*, 3998. [CrossRef]
38. Pica, A.; Guran, C.; Andronescu, E.; Oprea, O.; Ficai, D.; Ficai, A. Antimicrobial performances of some film forming materials based on silver nanoparticles. *J. Optoelectron. Adv. Mater.* **2012**, *14*, 863–868.
39. Nedelcu, I.A.; Ficai, A.; Sonmez, M.; Ficai, D.; Oprea, O.; Andronescu, E. Silver Based Materials for Biomedical Applications. *Curr. Org. Chem.* **2014**, *18*, 173–184. [CrossRef]

Chapter 5. General conclusions

Bacterial and fungal growth leads that spoil large food quantities can be controlled by the creation and development of antibacterial and antifungal packages. An important role preservation and safety is reserved to such antimicrobial packages. Our results but also literature studies support the conclusion that the antimicrobial packaging films prolong the latency stage and decrease the growth of fungi and bacteria, enhancing the quality and improving the safety of the food, prolonging also the shelf life. Introducing antimicrobials in the polymeric film for food packaging, the proliferation of the microorganisms is inhibited and as a consequence the shelf life is prolonged. As such, the safety and quality of vegetables, meat, dairy or fruits is ensured.

The state of the art in the field was documented based on several hundreds of papers and were also published in two extensive reviews one of them being published in Coatings (Q2) having 148 references and a second in Foods (Q1) having 289 references. Along with the two reviews, additional 4 papers published in ISI journals were published and these papers were related to additional references (~290 references). Based on such a comprehensive literature research, the PhD thesis continued with the implementation of the acquired information and with the development of the new, innovative solutions and packaging materials made from polymers that are biodegradable (e.g. alginate or chitosan). The packaging films were bestowed with antimicrobial properties by mixing the blend with zinc oxide or/and silver nanoparticles loaded with essential oil.

The quantity of commercially accessible antibacterial and antifungal packaging available is low, despite the high number of substances tested for their antimicrobial activity. In countries like US or Japan, as an exception, there are some packaging based on silver ions or nanoparticles. Such silver-based solutions for the antimicrobial packaging films are expected to be introduced also in E.U., especially as the silver was included as a food additive and a surface biocidal on the permitted provisional list. Therefore, use of silver nanoparticles in the antimicrobial packaging comes as a perfectly logical conclusion. Toxicity concerns permits only using low level of silver nanoparticles. To further decrease the amount of AgNPs used into the antimicrobial packaging we adopted a synergic approach. Therefore, beside silver nanoparticles, we have used also ZnO nanoparticles – a potent antimicrobial agent, that is classified as GRAS by FDA. ZnO is suitable to be introduced in films for food packaging as it has strong antibacterial and antifungal properties. When both types of nanoparticles are present into the packaging the antimicrobial activity is greatly enhanced due to the synergic action mechanisms. Each type of nanoparticle is sensitizing the microorganisms and it is making it more susceptible to the next attack. Adding more nanoparticles types into the polymeric matrix has enhanced the antimicrobial activity.

Plant extracts and especially essential oils have a high antimicrobial potential and can act also as antioxidant agents, therefore many research studies are concentrated on this topic. Among other substances, citronellal, citronellol and citral are the principal compounds found in citronella essential oil (CEO). By adding a third antimicrobial agent to the packaging films, such as a natural extract, the citronella essential oil, permits lowering of the amount of used nanoparticles due to the synergic action. US-FDA considers citronella essential oil as a biopesticide, non-toxic, that also exhibits strong antimicrobial properties.

US-FDA is classifying chitosan as a non-toxic and safe material (GRAS) that can be used in food industry. Despite chitosan exhibiting low barrier properties and a poor mechanical resistance,

it is intensely studied for edible packaging solutions. In fact, as a biopolymer is the most studied, as it is also very abundant. It is a polysaccharide, extracted from the shrimp-shells but also from mushroom stems, that exhibit antibacterial properties on Gram-negative bacterial strains.

When both type of nanoparticles were used, zinc oxide and silver, the films were exhibiting the strongest antimicrobial activity on the chosen strains. As explained before, this was attributed to the capacity to act in synergy for the film components. The presence of multiple inactivation pathways for microorganisms are probably the reason for the high antibacterial and antifungal activities obtained for this samples. Such mechanisms can include generation of the reactive oxygen species, electrostatic interaction with the cell wall, SPR effect of Ag nanoparticles, membrane rupture and nanoparticles internalization, as well as the citronella essential oil antibacterial and antifungal properties. The literature reports also synergic antimicrobial activities for some of these antimicrobials.

In conclusion, in the first study we have obtained chitosan –based packaging films, with silver and/or zinc oxide nanoparticles and essential oil from citronella. The use of up to four antimicrobials into the packaging composition has ensure strong and broad antibacterial and antifungal action on the tested strains. The high antimicrobial activity observed for chitosan – ZnO&Ag – citronella essential oil films makes them a viable packaging for fruits.

In the second study, we have obtained packaging films based on alginate / ZnO or Ag nanoparticles / citronella essential oil. The films are transparent, with a yellowish tint because of the interaction among CEO, ZnO nanoparticles and alginate. For alginate/Ag/ citronella essential oil films was observed a darkening effect correlated with the increase of Ag NPs content. For both type of alginate films the UV absorbance increased as the nanoparticles amount is higher. The transmittance for alginate/ZnO/ citronella essential oil films is under 5% in the 200–360 nm interval and under 10% in the 360–380 nm interval, but increases up to 88% in visible domain. In conclusion, the light barrier properties of a film are very important feature for a packaging. With a low UV transmittance, the packaging film can preserve some of the important nutrients (like proteins, lipids and vitamins) from high-energy photons induced photo-oxidation reactions.

Depending on the conditions storage (mainly light and temperature), in time, the films composed from alginate/Ag/ citronella essential oil can become more opaque. Is no surprise that in the films with an increasing silver quantity the absorbance change is larger. In addition, at room temperature the alginate – silver nanoparticles are transparent, but they have a tendency to darken when stored in the light presence at 30°C. In this case, when compared to the films stored at 4ºC for 6 days, the absorbance will go up with an additional 46% (from 32% to 78%). In conclusion, this feature can be useful to monitor the time and temperature conditions in which food was stored, like a time-temperature indicator. As shelf food must stay in-light, which means exposure time, such packaging feature can alert the customer if the food was exposed for too much time, or if the storage temperature was too high (practically a cumulative light and temperature indicator). The food freshness can be indicated by such packaging films.

The growth inhibition diameter values were obtained for four bacterial stains, relevant for foodborne infections: *Staphylococcus aureus* and *Bacillus cereus* as Gram-positive and for *Salmonella* Typhi and *Escherichia coli* as Gram-negative strains. The zinc oxide amount has a direct impact on the growth inhibition diameter for all four bacterial strains, the highest diameter being observed for the largest zinc oxide amount. The control zinc oxide sample, presented only a modest antibacterial effect. Only in the case of *Bacillus cereus* strain, a

significant value was obtained. In a similar way, plain citronella essential oil presented a smaller growth inhibition zone, but the antibacterial activity becomes important after adding zinc oxide nanoparticles. As such, a synergistic activity is suggested by these results, between zinc oxide and citronella essential oil.

Biofilm growth inhibition obtained values, showed that the samples present a strong activity against *Bacillus cereus* strain. For the highest silver content film, a strong Biofilm growth inhibition is observed. In conclusion we can hypothesized that in the case of biofilms the inhibition is in direct correlation with the concentration of the nanoparticles. According to the above results, these composite packaging films can be engineered for specific applications and/or microorganisms.

In conclusion, 21 innovative chitosan and alginate films were obtained, characterizes and their antimicrobial activities were determined. The chitosan and alginate composite films were tested as active food packaging. The antimicrobial assay results permit the conclusion that the mix of zinc oxide, silver nanoparticles and citronella essential oil has a strong antibacterial and antifungal activity, but also enhanced the water vapors or light barrier properties. Based on our results we can conclude that zinc oxide nanoparticles (presenting weak activity against *Candida albicans*) are sensitizing the microorganism for the citronella essential oil, so this can have a stronger antifungal effect. Increasing the amount of silver nanoparticles in the composite packaging improves even further the antimicrobial action.

As a general conclusion this type of membranes has a large spectrum of antibacterial and antifungal capacity and are suitable to be used as packaging for cheese, fruits or other foodstuff. The grapes stored in chitosan packaging films with both types of nanoparticles and essential oil presented only occasional brown spots on the berry's surface, with no further evolution or spoilage the berry, the grapes being successfully preserved up to 14 days. Preliminary test on soft cheese packaged in alginate based films has shown a good capacity of preservation, with samples softness, texture and color unchanged over two weeks. In addition, worth mention that the citronella essential oil scent is compatible with such foodstuff.

5.2 Perspectives

Novel packaging based on alginate with both zinc oxide and silver nanoparticles together with the essential oil are obtained and their assessment is undergoing. The use of both types of nanoparticles and CEO is permitting a decrease of antimicrobials quantities, while maintaining the large spectrum activity.

For the future, my aim is to obtain cellulose antimicrobial packaging, with lower nanoparticles amount. Preserving or enhancing the strong antibacterial and antifungal activities will require the direct use of the active components from essential oils, alone or in various mix, according to the packed foodstuff type.

In addition to further improve the barrier and mechanical properties of the packaging film I intend to study different polymers blends (chitosan+ alginate; chitosan + cellulose; alginate + cellulose, etc.).

Also, covalently bounded nanoparticles onto the polymer chains will be considered and could be a suitable approach to limit the migration of the nanoparticles as well as their cleavage.

List of publications

ISI articles

1- **Ludmila MOTELICA**, Luciana MARINOF, Alina HOLBAN, Bogdan Stefan VASILE, Anton FICAI. *Optical, photocatalytic and antibacterial properties of zinc oxide nanoparticles obtained by a solvothermal method.* U.P.B. Sci. Bull., Series B, Vol. 82, Iss. 1, Year 2020

2- **Ludmila MOTELICA**, Denisa FICAI, Ovidiu Cristian OPREA, Anton FICAI, Ecaterina ANDRONESCU. *Smart Food Packaging Designed by Nanotechnological and Drug Delivery Approaches*. Coatings 2020, 10(9), 806; doi: 10.3390/coatings10090806, Year 2020 **FI 3.236 Q2**

3- **Ludmila MOTELICA**, Denisa FICAI, Anton FICAI, Ovidiu Cristian OPREA, Durmis Alpaslan Kaya, Ecaterina ANDRONESCU. *Biodegradable Antimicrobial Food Packaging: Trends and Perspectives*. Foods 2020, 9(10), 1438; doi: 10.3390/foods9101438, Year 2020 **FI 5.561 Q1**

4- **Ludmila MOTELICA**, Denisa FICAI, Anton FICAI, Roxana-Doina TRUSCA, Cornelia-Ioana ILIE Ovidiu Cristian OPREA, Ecaterina ANDRONESCU. *Innovative Antimicrobial Chitosan/ZnO/Ag NPs/Citronella Essential Oil Nanocomposite Potential Coating for Grapes*. Foods 2020, 9(12), 1801, doi: 10.3390/foods9121801, Year 2020 **FI 5.561 Q1.**

5- **Ludmila MOTELICA,** Denisa FICAI, Anton FICAI, Roxana-Doina TRUSCA, Ovidiu Cristian OPREA, Ecaterina ANDRONESCU, Alina-Maria HOLBAN. *Biodegradable Alginate Films with ZnO Nanoparticles and Citronella Essential Oil—A Novel Antimicrobial Structure.* Pharmaceutics **2021**,13(7), 1020; doi: 10.3390/pharmaceutics13071020, Year 2021 **FI 6.525 Q1**

6- **Ludmila MOTELICA,** Denisa FICAI, Anton FICAI, Vladimir ENE, Ovidiu Cristian OPREA, Stefan Bogdan VASILE, Ecaterina ANDRONESCU, Alina Maria HOLBAN. *Antibacterial Biodegradable Films Based on Alginate with Silver Nanoparticles and Lemongrass Essential Oil–Innovative Packaging for Cheese*. Nanomaterials 2021, 11(9), 2377; https://doi.org/10.3390/nano11092377, Year 2021 **FI 5.719 Q1**

Participation on National Conferences

1- **Ludmila MOTELICA**, Luciana MARINOF, Alina HOLBAN, Bogdan Stefan VASILE, Anton FICAI. *Optical, photocatalytic, and antibacterial properties of zinc oxide nanoparticles obtained by a solvothermal method.* RICCCE 21st Romanian International Conference on Chemistry and Chemical Engineering Constanța - Mamaia Romania 2019

2- **Ludmila MOTELICA**, Luciana MARINOF, Alina HOLBAN, Bogdan Stefan VASILE, Anton FICAI. *Study on the optical, photocatalytic and antibacterial properties of zinc oxide nanoparticles (Romanian)*. Conferinţă- Aplicaţii ale chimiei in nanoştiinţe şi ingineria bionanomaterialelor, (AOSR), Bucureşti,16 July 2020.

3- Denisa FICAI, **Ludmila MOTELICA,** Gabriela PETRISOR, Irina FIERESCU, Radu Claudiu FIERESCU, Anton FICAI. *Porous materials in the treatment of microbiota-*

related diseases, smart functional nanomaterials: from synthesis to advanced applications (on-line) Rome, Italy 7-8 May 2021.

4- **Ludmila MOTELICA,** Denisa FICAI, Ovidiu Oprea, Anton FICAI, Roxana-Doina TRUSCA. Ecaterina Andronescu, Alina Maria HOLBAN. *Alginate films ZnO nanoparticles and citronella essntial oil – novel antimicrobial packaging for cheese* International Scientific Conference- Applications of chemistry in nanosciences and biomaterials engineering, (on-line) Bucureşti, 25-26 June 2021.

5- **Ludmila MOTELICA,** Denisa FICAI, Ovidiu Oprea, Anton FICAI, Roxana-Doina TRUSCA. Ecaterina Andronescu, Alina Maria HOLBAN. *Antibacterial Biodegradable Films Based on Alginate with Silver Nanoparticles and Lemongrass Essential Oil-Innovative Packanging for Cheese* International Scientific Conference- Applications of chemistry in nanosciences and biomaterials engineering, (on-line) Bucureşti, 25-26 November 2021.

Patent applications

1. Ovidiu Cristian Oprea, Anton FICAI, Denisa FICAI, **Ludmila MOTELICA**, Ecaterina ANDRONESCU, Roxana Doina TRUSCA. *Composition and process for treating paper, parchment or other writing media, for removing pathogens such as fungi, mold or bacteria (Romanian)*. Nr. OSIM: A/00798/21.05.2020
2. Ovidiu Cristian Oprea, Anton FICAI, Denisa FICAI, **Ludmila MOTELICA**, Ecaterina ANDRONESCU, Roxana Doina TRUSCA. *Compositions and process for treating leather objects for conferring antibacterial and antifungal activity (Romanian)*. Nr. OSIM: A/ 00794/ 24.06.2020.

Research project – team member

1- **Lib2Life** - Revitalization of libraries and cultural heritage through advanced technologies" - PN-III-P1-1.2-PCCDI-2017-0689 / 69PCCDI/2018/Lib2Life/P1 2018-2021.

2- **UPB - Proof of Concept 2020 –** *„ Cellulosic materials with antimicrobial activity"* - Project implementation during 01.02.2021-31.01.2023.

3- **NanoSafePack** - "Innovative packaging with antimicrobial activity for food safety" Nr. 573PED/2022 - PN-III-P2-2.1-PED-2021-3414.; 2022-2024

Other papers

1. **Ludmila MOTELICA**, Luminiţa CRACIUN, Ioana ARDELEAN, Mădălina Violeta IOANA. *"Non-destructive Analyses of 16th Century Documents"*. Revista de Chimie (Bucureşti) 70, nr.8, pag. 2798-2802; 2019
2. **Ludmila Motelica**, Aurelian Popescu, Anca-Gabriela Razvan, Ovidiu Oprea, Roxana-Doina Trusca, Bogdan-Stefan Vasile, Florina Dumitru and Alina-Maria Holban. *Facile Use of ZnO Nanopowders to Protect Old Manual Paper Documents*. Materials, 13(23), 5452, 2020, doi:10.3390/ma13235452, ISSN 1996-1944, **Q2 (IF 3.057)**
3. Irina Fierascu, Radu Claudiu Fierascu, Toma Fistos, **Ludmila Motelica**, Ovidiu Oprea, Adrian Nicoara, Anton Ficai, Alexandru Stirban, Maria-Similia Zgarciu. *Non-invasive*

microanalysis of a written page from the Romanian heritage: The Homiliary of Varlaam (Cazania lui Varlaam). Microchemical Journal (2021), doi: 10.1016/j.microc.2021.106345 **Q1 (IF 3.594).**

4. Alexa-Maria Croitoru, Yasin Karaçelebi, Elif Saatcioglu, Eray Altan, Songul Ulag, Huseyin Kıvanc Aydogan, Ali Sahin, **Ludmila Motelica**, Ovidiu Oprea, Bianca-Maria Tihauan, Roxana-Cristina Popescu, Diana Savu, Roxana Trusca, Denisa Ficai, Oguzhan Gunduz, Anton Ficai - *Electrically Triggered Drug Delivery from Novel Electrospun Poly (Lactic Acid)/Graphene Oxide/Quercetin Fibrous Scaffolds for Wound Dressing Aplication.* Pharmaceutics 2021, 13(7), 957, https://doi.org/10.3390/pharmaceutics13070957 **Q1 (IF), 4.421**
5. Otilia Chirca, Cornelia Bicleșanu, Anamaria Florescu, **Ludmila Motelica**, Alina Maria Holban, Alexandru Burcea - *Comparative study on adhesion to the dental structure of the total ceramic crown with different adhesive cements,* Revista Română de Materiale / Romanian Journal of Materials 2021, 51 (2), 309 – 318, **(IF), 0.542**
6. Angela Spoială, Cornelia-Ioana Ilie, Georgiana Dolete, Roxana-Doina Trușcă, **Ludmila Motelica**, Ovidiu-Cristian Oprea, Denisa Ficai, Anton Ficai, Ecaterina Andronescu, Lia-Mara Dițu - *The development of antimicrobial chitosan/zno nanocomposite membranes for water purification*, Revista Română de Materiale / Romanian Journal of Materials 2022, 52 (1), 17-25, **(IF), 0.542**
7. Gabriela Petrisor, **Ludmila Motelica**, Luminita Narcisa Craciun, Ovidiu Cristian Oprea Denisa Ficai and Anton Ficai - *Melissa officinalis: Composition, Pharmacological Effects and Derived Release Systems*—A Review Molecular Sciences 2022, 23(7), 3591; https://doi.org/10.3390/ijms23073591, **Q1 (IF), 5,924**
8. Gabriela Petrisor Denisa Ficai , **Ludmila Motelica** , Roxana Doina Trusca , Alexandra Cătălina Bîrcă, Bogdan St,efan Vasile, Georgeta Voicu, Ovidiu Cristian Oprea, Augustin Semenescu, Anton Ficai, Mircea Ionut Popitiu, Irina Fierascu, Radu Claudiu Fierascu, Elena Lacramioara Radu Lilia Matei, Laura Deisa Dragu, Ioana Madalina Pitica, Mihaela Economescu and Coralia Bleotu - *Mesoporous Silica Materials Loaded with Gallic Acid with Antimicrobial Potential Nanomaterials* 2022, 12(10), 1648; https://doi.org/10.3390/nano12101648, **Q1 (IF), 5.076**
9. Alexa-Maria Croitoru, Alina Morosan, Bianca Tihauan, Ovidiu Oprea **Ludmila Motelica**, Roxana Trusca, Adrian Ionut Nicoara, Roxana-Cristina Popescu, Diana Savu, Dan Eduard Mihaiescu and Anton Ficai - *Novel Graphene Oxide/Quercetin and Graphene Oxide/Juglone Nanostructured Platforms as Effective Drug Delivery Systems with Biomedical Applications* Nanomaterials 2022, 12(11), 1943; https://doi.org/10.3390/nano12111943, **Q1 (IF), 5.076**

REFERENCES

1. *Technical Platform on the Measurement and Reduction of Food Loss and Waste. Available online: http://www.fao.org/platform-food-loss-waste/en/.* accessed in 01.07.2021.
2. Ishangulyyev, S., S. Kim, and S.H. Lee, *Understanding Food Loss and Waste-Why Are We Losing and Wasting Food?* Foods, 2019. **8**(8): p. 297.
3. Jiang, B., et al., *Reutilization of Food Waste: One-Step Extration, Purification and Characterization of Ovalbumin from Salted Egg White by Aqueous Two-Phase Flotation.* Foods, 2019. **8**(8): p. 286.
4. *https://www.grandviewresearch.com/industry-analysis/food-packaging-market.* accessed in 26.09.2020.
5. Wohner, B., et al., *Environmental and economic assessment of food-packaging systems with a focus on food waste. Case study on tomato ketchup.* Science of the Total Environment, 2020. **738**.
6. *https://ec.europa.eu/environment/circular-economy/index_en.htm.* accessed 26.09.2020.
7. Makaremi, M., et al., *Safely Dissolvable and Healable Active Packaging Films Based on Alginate and Pectin.* Polymers, 2019. **11**(10): p. 1594.
8. Kaladharan, P., et al., *Marine plastic litter in certain trawl grounds along the peninsular coasts of India.* Marine Pollution Bulletin, 2020. **157**: p. 111299.
9. Chen, F.Y., et al., *Impact of regulatory focus on express packaging waste recycling behavior: moderating role of psychological empowerment perception.* Environmental Science and Pollution Research, 2019. **26**(9): p. 8862-8874.
10. White, A. and S. Lockyer, *Removing plastic packaging from fresh produce - what's the impact?* Nutrition Bulletin, 2020. **45**(1): p. 35-50.
11. Guo, J.J., et al., *Source, migration and toxicology of microplastics in soil.* Environment International, 2020. **137**: p. 105263.
12. Boz, Z., V. Korhonen, and C.K. Sand, *Consumer Considerations for the Implementation of Sustainable Packaging: A Review.* Sustainability, 2020. **12**(6): p. 2192.
13. Clark, N., R. Trimingham, and G.T. Wilson, *Incorporating Consumer Insights into the UK Food Packaging Supply Chain in the Transition to a Circular Economy.* Sustainability, 2020. **12**(15): p. 6106.
14. Zemljic, L.F., et al., *Physicochemical Characterization of Packaging Foils Coated by Chitosan and Polyphenols Colloidal Formulations.* International Journal of Molecular Sciences, 2020. **21**(2): p. 495.
15. Esmailzadeh, H., et al., *CuO/LDPE nanocomposite for active food packaging application: a comparative study of its antibacterial activities with ZnO/LDPE nanocomposite.* Polymer Bulletin, 2020. **https://doi.org/10.1007/s00289-020-03175-7**.
16. Zia, J., et al., *Low-density polyethylene/curcumin melt extruded composites with enhanced water vapor barrier and antioxidant properties for active food packaging.* Polymer, 2019. **175**: p. 137-145.
17. Habib, S., et al., *Preparation of Progressive Antibacterial LDPE Surface via Active Biomolecule Deposition Approach.* Polymers, 2019. **11**(10).
18. Giannakas, A., et al., *Novel LDPE/Chitosan Rosemary and Melissa Extract Nanostructured Active Packaging Films.* Nanomaterials, 2019. **9**(8): p. 1105.
19. Kuster-Boluda, A., N.V. Vila, and I. Kuster, *Managing international distributors' complaints: an exploratory study.* Journal of Business & Industrial Marketing, 2020. **https://doi.org/10.1108/JBIM-11-2018-0336**.
20. Kerry, J.P., M.N. O'Grady, and S.A. Hogan, *Past, current and potential utilisation of active and intelligent packaging systems for meat and muscle-based products: A review.* Meat Science, 2006. **74**(1): p. 113-130.
21. O' Callaghan, K.A.M. and J.P. Kerry, *Assessment of the antimicrobial activity of potentially active substances (nanoparticled and non-nanoparticled) against cheese-derived micro-organisms.* International Journal of Dairy Technology, 2014. **67**(4): p. 483-489.
22. Rai, M., et al., *Smart nanopackaging for theenhancement of foodshelf life.* Environmental Chemistry Letters, 2019. **17**(1): p. 277-290.
23. Vilas, C., M. Mauricio-Iglesias, and M.R. Garcia, *Model-based design of smart active packaging systems with antimicrobial activity.* Food Packaging and Shelf Life, 2020. **24**: p. 100446.
24. Jayasena, D.D. and C. Jo, *Essential oils as potential antimicrobial agents in meat and meat products: A review.* Trends in Food Science & Technology, 2013. **34**(2): p. 96-108.
25. Szabo, K., et al., *Active Packaging-Poly(Vinyl Alcohol) Films Enriched with Tomato By-Products Extract.* Coatings, 2020. **10**(2).
26. Souza, V.G.L., et al., *Eco-Friendly ZnO/Chitosan Bionanocomposites Films for Packaging of Fresh Poultry Meat.* Coatings, 2020. **10**(2): p. 110.
27. Shruthy, R., S. Jancy, and R. Preetha, *Cellulose nanoparticles synthesised from potato peel for the development of active packaging film for enhancement of shelf life of raw prawns (Penaeus monodon) during frozen storage.* International Journal of Food Science and Technology, 2020. **https://doi.org/10.1111/ijfs.14551**.

28. Han, J.H., *Antimicrobial food packaging*. Food Technology, 2000. **54**(3): p. 56-65.
29. Surendhiran, D., et al., *Fabrication of high stability active nanofibers encapsulated with pomegranate peel extract using chitosan/PEO for meat preservation.* Food Packaging and Shelf Life, 2020. **23**.
30. Settier-Ramirez, L., et al., *PVOH/protein blend films embedded with lactic acid bacteria and their antilisterial activity in pasteurized milk.* International Journal of Food Microbiology, 2020. **322**.
31. Ramos, M., et al., *Controlled Release of Thymol from Poly(Lactic Acid)-Based Silver Nanocomposite Films with Antibacterial and Antioxidant Activity.* Antioxidants, 2020. **9**(5).
32. Istrati, D., et al., *Phyto-mediated nanostructured carriers based on dual vegetable actives involved in the prevention of cellular damage.* Materials Science & Engineering C-Materials for Biological Applications, 2016. **64**: p. 249-259.
33. Lacatusu, I., et al., *Lipid nanocarriers based on natural compounds: An evolving role in plant extract delivery.* European Journal of Lipid Science and Technology, 2014. **116**(12): p. 1708-1717.
34. Caputo, L., et al., *Chemical Composition and Biological Activities of Essential Oils from Peels of Three Citrus Species.* Molecules, 2020. **25**(8): p. 1890.
35. Zhang, H.J. and J.Q. Wang, *Constituents of the Essential Oils of Garlic and Citronella and Their Vapor-phase Inhibition Mechanism against S.aureus.* Food Science and Technology Research, 2019. **25**(1): p. 65-74.
36. Francikowski, J., et al., *Commercially Available Essential Oil Formulas as Repellents Against the Stored-Product Pest Alphitobius diaperinus.* Insects, 2019. **10**(4): p. 96.
37. Go, E.J. and K.B. Song, *Effect of java citronella essential oil addition on the physicochemical properties of Gelidium corneum-chitosan composite films.* Food Science and Biotechnology, 2020. **29**(7): p. 909-915.
38. Nedelcu, I.A., et al., *Silver Based Materials for Biomedical Applications.* Current Organic Chemistry, 2014. **18**(2): p. 173-184.
39. Vaja, F., et al., *Effects of ZnO Nanoparticles on the Wet Scrub Resistance and Photocatalytic Properties of Acrylic Coatings.* Revista De Chimie, 2012. **63**(7): p. 722-726.
40. Kumar Santosh, et al., *Biodegradable Hybrid Nanocomposite of Chitosan/Gelatin and Green Synthesized Zinc Oxide Nanoparticles for Food Packaging.* Foods, 2020. **9**(9): p. 1143.
41. Wang, Y., et al., *Preparation of Chitosan/Corn Starch/Cinnamaldehyde Films for Strawberry Preservation.* Foods, 2019. **8**(9): p. 423.
42. Munteanu, S.B. and C. Vasile, *Vegetable Additives in Food Packaging Polymeric Materials.* Polymers, 2020. **12**(1): p. 28.
43. Valdes, A., et al., *Gelatin-Based Antimicrobial Films Incorporating Pomegranate (Punica granatum L.) Seed Juice by-Product.* Molecules, 2020. **25**(1): p. 166.
44. Becerril, R., C. Nerin, and F. Silva, *Encapsulation Systems for Antimicrobial Food Packaging Components: An Update.* Molecules, 2020. **25**(5): p. 1134.
45. Naidu, D.S. and M.J. John, *Effect of Clay Nanofillers on the Mechanical and Water Vapor Permeability Properties of Xylan-Alginate Films.* Polymers, 2020. **12**(10).
46. Motelica, L., et al., *Innovative Antimicrobial Chitosan/ZnO/Ag NPs/Citronella Essential Oil Nanocomposite - Potential Coating for Grapes.* Foods, 2020. **9**(12): p. 1801.
47. Youssef, A.M. and S.M. El-Sayed, *Bionanocomposites materials for food packaging applications: Concepts and future outlook.* Carbohydrate Polymers, 2018. **193**: p. 19-27.
48. Krepker, M., et al., *Active food packaging films with synergistic antimicrobial activity.* Food Control, 2017. **76**: p. 117-126.
49. Sanches-Silva, A., et al., *Trends in the use of natural antioxidants in active food packaging: a review.* Food Additives and Contaminants Part a-Chemistry Analysis Control Exposure & Risk Assessment, 2014. **31**(3): p. 374-395.
50. Dainelli, D., et al., *Active and intelligent food packaging: legal aspects and safety concerns.* Trends in Food Science & Technology, 2008. **19**: p. 10.
51. Realini, C.E. and B. Marcos, *Active and intelligent packaging systems for a modern society.* Meat Science, 2014. **98**(3): p. 404-419.
52. Lee, S.J. and A.T.M.M. Rahman, *Intelligent Packaging for Food Products.* Innovations in Food Packaging, 2nd Edition, 2014: p. 171-209.
53. Galagan, Y. and W.F. Su, *Fadable ink for time-temperature control of food freshness: Novel new time-temperature indicator.* Food Research International, 2008. **41**(6): p. 653-657.
54. Taoukis, P.S. and T.P. Labuza, *Applicability of Time-Temperature Indicators as Shelf-Life Monitors of Food-Products.* Journal of Food Science, 1989. **54**(4): p. 783-788.
55. Fang, Z.X., et al., *Active and intelligent packaging in meat industry.* Trends in Food Science & Technology, 2017. **61**: p. 60-71.
56. Wang, S.D., et al., *Review of Time Temperature Indicators as Quality Monitors in Food Packaging.* Packaging Technology and Science, 2015. **28**(10): p. 839-867.
57. Yoshida, C.M.P., et al., *Chitosan biobased and intelligent films: Monitoring pH variations.* Lwt-Food Science and Technology, 2014. **55**(1): p. 83-89.

58. Safarik, I., et al., *Potential of magnetically responsive (nano)biocomposites.* Soft Matter, 2012. **8**(20): p. 5407-5413.
59. Arvanitoyannis, I.S. and A.C. Stratakos, *Fresh and Processed Meat and Meat Products.* Modified Atmosphere and Active Packaging Technologies, 2012: p. 223-259.
60. Arvanitoyannis, I.S. and A.C. Stratakos, *Application of Modified Atmosphere Packaging and Active/Smart Technologies to Red Meat and Poultry: A Review.* Food and Bioprocess Technology, 2012. **5**(5): p. 1423-1446.
61. Umuhumuza, L.C. and X.L. Sun, *Rapid detection of pork meat freshness by using L-cysteine-modified gold electrode.* European Food Research and Technology, 2011. **232**(3): p. 425-431.
62. Matindoust, S., et al., *Food quality and safety monitoring using gas sensor array in intelligent packaging.* Sensor Review, 2016. **36**(2): p. 169-183.
63. Vermeiren, L., et al., *Developments in the active packaging of foods.* Trends in Food Science & Technology, 1999. **10**(3): p. 77-86.
64. Chaix, E., C. Guillaume, and V. Guillard, *Oxygen and Carbon Dioxide Solubility and Diffusivity in Solid Food Matrices: A Review of Past and Current Knowledge.* Comprehensive Reviews in Food Science and Food Safety, 2014. **13**(3): p. 261-286.
65. Sun, L., et al., *A Practical Multivariable Control Approach Based on Inverted Decoupling and Decentralized Active Disturbance Rejection Control.* Industrial & Engineering Chemistry Research, 2016. **55**(7): p. 2008-2019.
66. Ehsan M and L. M., *Intelligent packaging in meat industry: An overview of existing solutions.* Food Sci Technol, 2014.
67. Bolumar, T., M.L. Andersen, and V. Orlien, *Antioxidant active packaging for chicken meat processed by high pressure treatment.* Food Chemistry, 2011. **129**(4): p. 1406-1412.
68. Liu, L., et al., *Development of Time-Temperature Data Collection Program for Frozen Fish in the Cold Chain.* Sensor Letters, 2010. **8**(1): p. 47-51.
69. Gomez-Estaca, J., et al., *Advances in antioxidant active food packaging.* Trends in Food Science & Technology, 2014. **35**(1): p. 42-51.
70. Feng, K., et al., *Enhancement of the antimicrobial activity of cinnamon essential oil-loaded electrospun nanofilm by the incorporation of lysozyme.* Rsc Advances, 2017. **7**(3): p. 1572-1580.
71. Ahmed, J., M. Mulla, and Y.A. Arfat, *Application of high-pressure processing and polylactide/cinnamon oil packaging on chicken sample for inactivation and inhibition of Listeria monocytogenes and Salmonella Typhimurium, and post-processing film properties.* Food Control, 2017. **78**: p. 160-168.
72. Gomez-Estaca, J., et al., *Development, properties, and stability of antioxidant shrimp muscle protein films incorporating carotenoid-containing extracts from food by-products.* Lwt-Food Science and Technology, 2015. **64**(1): p. 189-196.
73. Bolumar, T., et al., *Rosemary and oxygen scavenger in active packaging for prevention of high-pressure induced lipid oxidation in pork patties.* Food Packaging and Shelf Life, 2016. **7**: p. 26-33.
74. He, S.K., et al., *Antimicrobial Efficiency of Chitosan Solutions and Coatings Incorporated with Clove Oil and/or Ethylenediaminetetraacetate.* Journal of Food Safety, 2014. **34**(4): p. 345-352.
75. Fratianni, F., et al., *Preservation of Chicken Breast Meat Treated with Thyme and Balm Essential Oils.* Journal of Food Science, 2010. **75**(8): p. M528-M535.
76. Mulla, M., et al., *Antimicrobial efficacy of clove essential oil infused into chemically modified LLDPE film for chicken meat packaging.* Food Control, 2017. **73**: p. 663-671.
77. Zhang, S.B., et al., *New insights into synergistic antimicrobial and antifouling cotton fabrics via dually finished with quaternary ammonium salt and zwitterionic sulfobetaine.* Chemical Engineering Journal, 2018. **336**: p. 123-132.
78. Singh, S., et al., *Antibacterial and amine scavenging properties of silver-silica composite for post-harvest storage of fresh fish.* Food and Bioproducts Processing, 2018. **107**: p. 61-69.
79. Shankar, S. and J.W. Rhim, *Antimicrobial wrapping paper coated with a ternary blend of carbohydrates (alginate, carboxymethyl cellulose, carrageenan) and grapefruit seed extract.* Carbohydrate Polymers, 2018. **196**: p. 92-101.
80. Lu, P., et al., *Application of Nanofibrillated Cellulose on BOPP/LDPE Film as Oxygen Barrier and Antimicrobial Coating Based on Cold Plasma Treatment.* Coatings, 2018. **8**(6).
81. Zhu, R.N., et al., *An approach for reinforcement of paper with high strength and barrier properties via coating regenerated cellulose.* Carbohydrate Polymers, 2018. **200**: p. 100-105.
82. Zhang, X.M., et al., *One-step coagulation to construct durable anti-fouling and antibacterial cellulose film exploiting Ag@AgCl nanoparticle- triggered photo-catalytic degradation.* Carbohydrate Polymers, 2018. **181**: p. 499-505.
83. Shankar, S., A.A. Oun, and J.W. Rhim, *Preparation of antimicrobial hybrid nano-materials using regenerated cellulose and metallic nanoparticles.* International Journal of Biological Macromolecules, 2018. **107**: p. 17-27.

84. Salari, M., et al., *Development and evaluation of chitosan based active nanocomposite films containing bacterial cellulose nanocrystals and silver nanoparticles.* Food Hydrocolloids, 2018. **84**: p. 414-423.
85. Srikandace, Y., et al., *Antibacterial activity of bacterial cellulose-based edible film incorporated with Citrus spp essential oil.* 2nd International Symposium on Green Technology for Value Chains 2017 (Greenvc 2017), 2018. **160**.
86. Yousefi, M., M. Azizi, and A. Ehsani, *Antimicrobial coatings and films on meats: A perspective on the application of antimicrobial edible films or coatings on meats from the past to future.* Bali Medical Journal, 2018. **7**(1): p. 87-96.
87. Wang, H.X., J. Qan, and F.Y. Ding, *Emerging Chitosan-Based Films for Food Packaging Applications.* Journal of Agricultural and Food Chemistry, 2018. **66**(2): p. 395-413.
88. Priyadarshi, R., et al., *Chitosan film incorporated with citric acid and glycerol as an active packaging material for extension of green chilli shelf life.* Carbohydrate Polymers, 2018. **195**: p. 329-338.
89. Yun, Y.H., et al., *Preparation of chitosan/polyvinyl alcohol blended films containing sulfosuccinic acid as the crosslinking agent using UV curing process.* Food Research International, 2017. **100**: p. 377-386.
90. Nancy Robledo1, L.L., Andrea Bunger1, Cristian Tapia1,Lilian Abugoch1, *Effects of Antimicrobial Edible Coating of Thymol Nanoemulsion/Quinoa Protein/Chitosan on the Safety, Sensorial Properties, and Quality of Refrigerated Strawberries (Fragaria × ananassa) Under Commercial Storage Environment.* Food and Bioprocess Technology (2018) 2018.
(https://doi.org/10.1007/s11947-018-2124-3): p. 1566–1574.
91. Sogut, E. and A.C. Seydim, *Development of Chitosan and Polycaprolactone based active bilayer films enhanced with nanocellulose and grape seed extract.* Carbohydrate Polymers, 2018. **195**: p. 180-188.
92. Jiawei Yan, Z.L., Zhaojun Ban, Hongyan Lu, Dong Li, Dongmei Yang, Morteza Soleimani Aghdam, Li Li *The effect of the layer-by-layer (LBL) edible coating on strawberry qualityand metabolites during storage.* 2019. **147**: p. 29-38.
93. Ye, J.S., et al., *Preparation and properties of polylactic acid-tea polyphenol-chitosan composite membranes.* International Journal of Biological Macromolecules, 2018. **117**: p. 632-639.
94. Uranga, J., et al., *Citric acid-incorporated fish gelatin/chitosan composite films.* Food Hydrocolloids, 2019. **86**: p. 95-103.
95. Soni, B., et al., *Physicochemical, antimicrobial and antioxidant properties of chitosan/TEMPO biocomposite packaging films.* Food Packaging and Shelf Life, 2018. **17**: p. 73-79.
96. Yang, W., et al., *Polyvinyl alcohol/chitosan hydrogels with enhanced antioxidant and antibacterial properties induced by lignin nanoparticles.* Carbohydrate Polymers, 2018. **181**: p. 275-284.
97. Kaewklin, P., et al., *Active packaging from chitosan-titanium dioxide nanocomposite film for prolonging storage life of tomato fruit.* International Journal of Biological Macromolecules, 2018. **112**: p. 523-529.
98. Zheng, K.W., et al., *Physical, antibacterial and antioxidant properties of chitosan films containing hardleaf oatchestnut starch and Litsea cubeba oil.* International Journal of Biological Macromolecules, 2018. **118**: p. 707-715.
99. Zhang, Z.J., et al., *Preparation and characterization of biocomposite chitosan film containing Perilla frutescens (L.) Britt. essential oil.* Industrial Crops and Products, 2018. **112**: p. 660-667.
100. Priyadarshi, R., et al., *Chitosan films incorporated with Apricot (Prunus armeniaca) kernel essential oil as active food packaging material.* Food Hydrocolloids, 2018. **85**: p. 158-166.
101. Ojagh, S.M., et al., *Effect of chitosan coatings enriched with cinnamon oil on the quality of refrigerated rainbow trout.* Food Chemistry, 2010. **120**(1): p. 193-198.
102. Xing, Y.G., et al., *Effect of Chitosan Coating with Cinnamon Oil on the Quality and Physiological Attributes of China Jujube Fruits.* Biomed Research International, 2015: p. 835151.
103. Wang, Q.Y., et al., *Effect of chitosan-carvacrol coating on the quality of Pacific white shrimp during iced storage as affected by caprylic acid.* International Journal of Biological Macromolecules, 2018. **106**: p. 123-129.
104. Peretto, G., et al., *Optimization of Antimicrobial and Physical Properties of Alginate Coatings Containing Carvacrol and Methyl Cinnamate for Strawberry Application.* Journal of Agricultural and Food Chemistry, 2014. **62**(4): p. 984-990.
105. Borkowski, D., I. Krucinska, and Z. Draczynski, *Preparation of Nanocomposite Alginate Fibers Modified with Titanium Dioxide and Zinc Oxide.* Polymers, 2020. **12**(5): p. 1040.
106. Fahmy, A., et al., *Molecular properties of polyvinyl alcohol/sodium alginate composite.* Biointerface Research in Applied Chemistry, 2020. **10**(1): p. 4734-4739.
107. Senturk Parreidt, T., K. Muller, and M. Schmid, *Alginate-Based Edible Films and Coatings for Food Packaging Applications.* Foods, 2018. **7**(10).
108. Vizzini, P., et al., *Development and Evaluation of qPCR Detection Method and Zn-MgO/Alginate Active Packaging for Controlling Listeria monocytogenes Contamination in Cold-Smoked Salmon.* Foods, 2020. **9**(10).
109. Paduraru, A., et al., *Antimicrobial Wound Dressings as Potential Materials for Skin Tissue Regeneration.* Materials, 2019. **12**(11).

110. Anugrah, D.S.B., et al., *A Review of Polysaccharide-Zinc Oxide Nanocomposites as Safe Coating for Fruits Preservation.* Coatings, 2020. **10**(10).
111. Avramescu, S.M., et al., *Edible and Functionalized Films/Coatings-Performances and Perspectives.* Coatings, 2020. **10**(7): p. 687.
112. Bakil, S.N.A., et al., *Sodium Alginate-Zinc Oxide Nanocomposite Film for Antibacterial Wound Healing Applications.* Biointerface Research in Applied Chemistry, 2020. **10**(5): p. 6289-6296.
113. Khare, S., et al., *Effects of ingested nanocellulose on intestinal microbiota and homeostasis in Wistar Han rats.* Nanoimpact, 2020. **18**.
114. DeLoid, G.M., et al., *Toxicological effects of ingested nanocellulose in in vitro intestinal epithelium and in vivo rat models.* Environmental Science-Nano, 2019. **6**(7): p. 2105-2115.
115. Chen, Y.J., et al., *Subchronic exposure to cellulose nanofibrils induces nutritional risk by non-specifically reducing the intestinal absorption.* Carbohydrate Polymers, 2020. **229**.
116. Dimitrijevic, M., et al., *Safety aspects of nanotechnology applications in food packaging.* 58th International Meat Industry Conference (Meatcon2015), 2015. **5**: p. 57-60.
117. dos Santos, C.A., A.P. Ingle, and M. Rai, *The emerging role of metallic nanoparticles in food.* Applied Microbiology and Biotechnology, 2020. **104**(6): p. 2373-2383.
118. Doskocz, N., et al., *Ecotoxicity of selected nanoparticles in relation to micro-organisms in the water ecosystem.* Desalination and Water Treatment, 2020. **186**: p. 50-55.
119. Noori, A., et al., *Silver nanoparticle detection and accumulation in tomato (Lycopersicon esculentum).* Journal of Nanoparticle Research, 2020. **22**(6).
120. Dash, S.R. and C.N. Kundu, *Promising opportunities and potential risk of nanoparticle on the society.* Iet Nanobiotechnology, 2020. **14**(4): p. 253-260.
121. Garcia, C.V., G.H. Shin, and J.T. Kim, *Metal oxide-based nanocomposites in food packaging: Applications, migration, and regulations.* Trends in Food Science & Technology, 2018. **82**: p. 21-31.
122. Souza, V.G.L. and A.L. Fernando, *Nanoparticles in food packaging: Biodegradability and potential migration to food-A review.* Food Packaging and Shelf Life, 2016. **8**: p. 63-70.
123. Istiqola, A. and A. Syafiuddin, *A review of silver nanoparticles in food packaging technologies: Regulation, methods, properties, migration, and future challenges.* Journal of the Chinese Chemical Society, 2020. **https://doi.org/10.1002/jccs.202000179**.
124. Sahoo, R.K., *Packaging: Polymer-Metal-Based Micro- and Nanocomposites.* Encyclopedia of Polymer Applications, Vols I-Iii, 2019: p. 2021-2040.
125. Morais, L.D., et al., *Critical evaluation of migration studies of silver nanoparticles present in food packaging: a systematic review.* Critical Reviews in Food Science and Nutrition, 2019.
126. Ramachandran, R., et al., *In vivo toxicity evaluation of biologically synthesized silver nanoparticles and gold nanoparticles on adult zebrafish: a comparative study.* 3 Biotech, 2018. **8**(10).
127. Zhou, Q.F., et al., *Determination and characterization of metal nanoparticles in clams and oysters.* Ecotoxicology and Environmental Safety, 2020. **198**.
128. Gong, Y., et al., *Bioaccumulation and human health risk of shellfish contamination to heavy metals and As in most rapid urbanized Shenzhen, China.* Environmental Science and Pollution Research, 2020. **27**(2): p. 2096-2106.
129. Shah, N., et al., *Monitoring Bioaccumulation (in Gills and Muscle Tissues), Hematology, and Genotoxic Alteration in Ctenopharyngodon idella Exposed to Selected Heavy Metals.* Biomed Research International, 2020. **2020**.
130. Wu, J., et al., *Foliar versus root exposure of AgNPs to lettuce: Phytotoxicity, antioxidant responses and internal translocation.* Environmental Pollution, 2020. **261**.
131. Becaro, A.A., et al., *Cytotoxic and genotoxic effects of silver nanoparticle/carboxymethyl cellulose on Allium cepa.* Environmental Monitoring and Assessment, 2017. **189**(7).
132. Ma, C.X., et al., *Dual roles of glutathione in silver nanoparticle detoxification and enhancement of nitrogen assimilation in soybean (Glycine max(L.) Merrill).* Environmental Science-Nano, 2020. **7**(7): p. 1954-1966.
133. Yang, Z.Z., et al., *Effects of Copper Oxide Nanoparticles on the Growth of Rice (Oryza Sativa L.) Seedlings and the Relevant Physiological Responses.* International Journal of Environmental Research and Public Health, 2020. **17**(4).
134. Yusefi-Tanha, E., et al., *Particle size and concentration dependent toxicity of copper oxide nanoparticles (CuONPs) on seed yield and antioxidant defense system in soil grown soybean (Glycine max cv. Kowsar).* Science of the Total Environment, 2020. **715**.
135. Rajput, V., et al., *ZnO and CuO nanoparticles: a threat to soil organisms, plants, and human health.* Environmental Geochemistry and Health, 2020. **42**(1): p. 147-158.
136. Rajput, V., et al., *Toxicity of copper oxide nanoparticles on spring barley (Hordeum sativum distichum).* Science of the Total Environment, 2018. **645**: p. 1103-1113.
137. Baskar, V., et al., *A comparative study of phytotoxic effects of metal oxide (CuO, ZnO and NiO) nanoparticles on in-vitro grown Abelmoschus esculentus.* Plant Biosystems, 2020. **https://doi.org/10.1080/11263504.2020.1753843**.

138. Jeon, Y.R., J. Yu, and S.J. Choi, *Fate Determination of ZnO in Commercial Foods and Human Intestinal Cells*. International Journal of Molecular Sciences, 2020. **21**(2).
139. Pereira, F.F., et al., *The Effect of ZnO Nanoparticles Morphology on the Toxicity Towards Microalgae Pseudokirchneriella subcapitata*. Journal of Nanoscience and Nanotechnology, 2020. **20**(1): p. 48-63.
140. Vasile, O.R., et al., *Influence of the size and the morphology of ZnO nanoparticles on cell viability*. Comptes Rendus Chimie, 2015. **18**(12): p. 1335-1343.
141. Voss, L., et al., *Environmental Impact of ZnO Nanoparticles Evaluated by in Vitro Simulated Digestion*. Acs Applied Nano Materials, 2020. **3**(1): p. 724-733.
142. Meng, J., et al., *Exposure to low dose ZnO nanoparticles induces hyperproliferation and malignant transformation through activating the CXCR2/NF-kappa B/ STAT3/ERK and AKT pathways in colonic mucosal cells*. Environmental Pollution, 2020. **263**.
143. Musial, J., et al., *Titanium Dioxide Nanoparticles in Food and Personal Care Products-What Do We Know about Their Safety?* Nanomaterials, 2020. **10**(6).
144. Kurtz, C.C., et al., *Acute high-dose titanium dioxide nanoparticle exposure alters gastrointestinal homeostasis in mice*. Journal of Applied Toxicology, 2020. **40**(10): p. 1384-1395.
145. Hashem, M.M., et al., *The long-term oral exposure to titanium dioxide impaired immune functions and triggered cytotoxic and genotoxic impacts in rats*. Journal of Trace Elements in Medicine and Biology, 2020. **60**.
146. Cao, X.Q., et al., *Foodborne Titanium Dioxide Nanoparticles Induce Stronger Adverse Effects in Obese Mice than Non-Obese Mice: Gut Microbiota Dysbiosis, Colonic Inflammation, and Proteome Alterations*. Small, 2020. **https://doi.org/10.1002/smll.202001858**.
147. Bettencourt, A., et al., *Analysis of the Characteristics and Cytotoxicity of Titanium Dioxide Nanomaterials Following Simulated In Vitro Digestion*. Nanomaterials, 2020. **10**(8).
148. Shi, L.E., et al., *Synthesis, antibacterial activity, antibacterial mechanism and food applications of ZnO nanoparticles: a review*. Food Additives and Contaminants Part a-Chemistry Analysis Control Exposure & Risk Assessment, 2014. **31**(2): p. 173-186.
149. McClements, D.J. and H. Xiao, *Is nano safe in foods? Establishing the factors impacting the gastrointestinal fate and toxicity of organic and inorganic food-grade nanoparticles*. Science of Food, 2017. **1**: p. 6.
150. Lee, C.C., et al., *Exposure to ZnO/TiO(2)Nanoparticles Affects Health Outcomes in Cosmetics Salesclerks*. International Journal of Environmental Research and Public Health, 2020. **17**(17).
151. Deyab, M.A., A.A. Nada, and A. Hamdy, *Comparative study on the corrosion and mechanical properties of nano-composite coatings incorporated with TiO2 nano-particles, TiO2 nano-tubes, and ZnO nano-flowers*. Progress in Organic Coatings, 2017. **105**: p. 245-251.
152. Motelica, L., et al., *Biodegradable Antimicrobial Food Packaging: Trends and Perspectives*. Foods, 2020. **9**(10): p. 1438.
153. Vasile, B.S., et al., *Synthesis and characterization of a novel controlled release zinc oxide/gentamicin-chitosan composite with potential applications in wounds care*. International Journal of Pharmaceutics, 2014. **463**(2): p. 161-169.
154. Sahu, D., et al., *Nanosized zinc oxide induces toxicity in human lung cells*. ISRN Toxicol, 2013. **2013**: p. 316075.
155. Sruthi, S., J. Ashtami, and P.V. Mohanan, *Biomedical application and hidden toxicity of Zinc oxide nanoparticles*. Materials Today Chemistry, 2018. **10**: p. 175-186.
156. Vandebriel, R.J. and W.H. De Jong, *A review of mammalian toxicity of ZnO nanoparticles*. Nanotechnol Sci Appl, 2012. **5**: p. 61-71.
157. El Shemy, M.A., N.I. Azab, and R.F. Salim, *Zinc Oxide Nanoparticles: The Hidden Danger*. International Journal of Biochemistry, Biophysics & Molecular Biology 2017. **2**(1): p. 1-9.
158. Mohammed, Y.H., et al., *Support for the Safe Use of Zinc Oxide Nanoparticle Sunscreens: Lack of Skin Penetration or Cellular Toxicity after Repeated Application in Volunteers*. Journal of Investigative Dermatology, 2019. **139**(2): p. 308-315.
159. Wright, P. and N. Jackson, *Safety of engineered nanomaterials and occupational health and safety issues for commercial scale production*, in *Handbook of clinical nanomedicine: law, business, regulation, safety, and risk*, R. Bawa, G. Audette, and B. Reese, Editors. 2016, Pan Stanford Publishing: Singapore. p. 569-619.
160. Reshma, V.G. and P.V. Mohanan, *Cellular interactions of zinc oxide nanoparticles with human embryonic kidney (HEK 293) cells*. Colloids and Surfaces B-Biointerfaces, 2017. **157**: p. 182-190.
161. Feltis, B.N., et al., *Independent cytotoxic and inflammatory responses to zinc oxide nanoparticles in human monocytes and macrophages*. Nanotoxicology, 2012. **6**(7): p. 757-765.
162. Alaraby, M., et al., *A comprehensive study of the harmful effects of ZnO nanoparticles using Drosophila melanogaster as an in vivo model*. Journal of Hazardous Materials, 2015. **296**: p. 166-174.
163. Wright, P.F.A., *Realistic Exposure Study Assists Risk Assessments of ZnO Nanoparticle Sunscreens and Allays Safety Concerns*. Journal of Investigative Dermatology, 2019. **139**(2): p. 277-278.

164. Radulescu, M., et al., *Antimicrobial coatings based on zinc oxide and orange oil for improved bioactive wound dressings and other applications.* Romanian Journal of Morphology and Embryology, 2016. **57**(1): p. 107-114.
165. Najnin, H., et al., *Biochemical and toxicological analysis of Cinnamomum tamala essential oil in Wistar rats.* Journal of Food Processing and Preservation, 2020. **44**(2).
166. Costa, W.K., et al., *Essential oil from Eugenia stipitata McVaugh leaves has antinociceptive, anti-inflammatory and antipyretic activities without showing toxicity in mice.* Industrial Crops and Products, 2020. **144**.
167. Bonin, E., et al., *Baccharis dracunculifolia: Chemical constituents, cytotoxicity and antimicrobial activity.* Lwt-Food Science and Technology, 2020. **120**.
168. Abou Baker, D.H., M. Al-Moghazy, and A.A.A. ElSayed, *The in vitro cytotoxicity, antioxidant and antibacterial potential of Satureja hortensis L. essential oil cultivated in Egypt.* Bioorganic Chemistry, 2020. **95**.
169. Tadtong, S., R. Watthanachaiyingcharoen, and N. Kamkaen, *Antimicrobial Constituents and Synergism Effect of the Essential Oils from Cymbopogon citratus and Alpinia galanga.* Natural Product Communications, 2014. **9**(2): p. 277-280.
170. Budiati, T., et al., *Antimicrobial activity of essential oil from Indonesian medicinal plants against food-borne pathogens.* 1st International Conference on Food and Agriculture 2018, 2018. **207**.
171. De Silva, B.C.J., et al., *Comparative in vitro efficacy of eight essential oils as antibacterial agents against pathogenic bacteria isolated from pet-turtles.* Veterinarni Medicina, 2018. **63**(7): p. 335-343.
172. Serb, M.D., et al., *Study of thermal decomposition of a zinc(II) monomethyl terephthalate complex, [Zn(CH3O-CO-C6H4COO)(2)(OH2)(3)]center dot 2H(2)O.* Journal of Thermal Analysis and Calorimetry, 2015. **121**(2): p. 691-695.
173. Vasile, O.R., et al., *Synthesis and characterization of nanostructured zinc oxide particles synthesized by the pyrosol method.* Journal of Nanoparticle Research, 2012. **14**(12).
174. Oprea, O., et al., *The Influence of the Thermal Treatment on Luminescence Properties of Zno.* Digest Journal of Nanomaterials and Biostructures, 2013. **8**(2): p. 747-756.
175. Oprea, O., et al., *Synthesis and characterization of ZnO nanostructures obtained in mixtures of ionic liquids with organic solvents.* Central European Journal of Chemistry, 2014. **12**(7): p. 749-756.
176. Oprea, O., et al., *Photoluminescence, Magnetic Properties and Photocatalytic Activity of Gd3+ Doped Zno Nanoparticles.* Digest Journal of Nanomaterials and Biostructures, 2012. **7**(4): p. 1757-1766.
177. Voicu, G., et al., *Antibacterial Activity of Zinc Oxide - Gentamicin Hybrid Material.* Digest Journal of Nanomaterials and Biostructures, 2013. **8**(3): p. 1191-1203.
178. Radulescu, M., et al., *Advances in Drug Delivery Systems, from 0 to 3D Superstructures.* Current Drug Targets, 2018. **19**(4): p. 393-405.
179. Ficai, D., et al., *Metal Oxide Nanoparticles: Potential Uses in Biomedical Applications.* Current Proteomics, 2014. **11**(2): p. 139-149.
180. Oprea, O., et al., *ZnO Applications and Challenges.* Current Organic Chemistry, 2014. **18**(2): p. 192-203.
181. Pica, A., et al., *Antimicrobial performances of some film forming materials based on silver nanoparticles.* Journal of Optoelectronics and Advanced Materials, 2012. **14**(9-10): p. 863-868.
182. Vasile, B.S., et al., *Wound Dressings Coated with Silver Nanoparticles and Essential Oils for The Management of Wound Infections.* Materials, 2020. **13**(7): p. 1682.
183. Khalir, W.K.A.W.M., et al., *In-Situ Biofabrication of Silver Nanoparticles inCeiba pentandraNatural Fiber UsingEntada spiralisExtract with Their Antibacterial and Catalytic Dye Reduction Properties.* Nanomaterials, 2020. **10**(6): p. 1104.
184. Nechifor, A.C., et al., *Removing of the Sulfur Compounds by Impregnated Polypropylene Fibers with Silver Nanoparticles-Cellulose Derivatives for Air Odor Correction.* Membranes, 2021. **11**(4): p. 256.
185. Kukushkina, E.A., et al., *Ag-Based Synergistic Antimicrobial Composites. A Critical Review.* Nanomaterials, 2021. **11**(7): p. 1687.
186. Lacatusu, I., et al., *New cosmetic formulations with broad photoprotective and antioxidative activities designed by amaranth and pumpkin seed oils nanocarriers.* Industrial Crops and Products, 2018. **123**: p. 424-433.
187. Mihaly, M., I. Lacatusu, and A. Meghea, *Sulphonephtalein chromophore as molecular probe in micelle systems.* Revista De Chimie, 2007. **58**(9): p. 929-932.
188. Niculae, G., et al., *Coencapsulation of Butyl-Methoxydibenzoylmethane and Octocrylene into Lipid Nanocarriers: UV Performance, Photostability and in vitro Release.* Photochemistry and Photobiology, 2013. **89**(5): p. 1085-1094.
189. Ipe, D.S., et al., *Silver Nanoparticles at Biocompatible Dosage Synergistically Increases Bacterial Susceptibility to Antibiotics.* Frontiers in Microbiology, 2020. **11**: p. 1074.
190. Mazur, P., et al., *Synergistic ROS-Associated Antimicrobial Activity of Silver Nanoparticles and Gentamicin Against Staphylococcus epidermidis.* International Journal of Nanomedicine, 2020. **15**: p. 3551-3562.